REMARKS

Claims 16, 17, 19, 20, 22, and 34 – 38 are pending in the application. Claims 16, 19 and 22 have been amended. Claims 1 – 15, 18, 21, and 23 – 33 have been cancelled. No new claims have been added. No new matter has been added.

Support for the amendment to claims 16, 19 and 22 can be found in the specification, for example at page 6, line 12 or on page 9, line 26.

Rejection of Claims 35 - 38 Under 35 USC 112, Second Paragraph

Claims 16, 17, 19, 20, 22 and 33 - 38 remain rejected under 35 USC 112, first paragraph. The Examiner alleges that the specification "while being enabling for a method of killing a cell in vivo using direct delivery of the adenovirus to the cell and a method of killing a cell in vitro, does not reasonably provide enablement for a method of killing a cell in vivo using a genus of administration routes." (Office Action, p.2). Applicants respectfully traverse the rejection.

The instant claims recite a method of killing a cell that is sensitive to DT-A or PEA, comprising infecting the cell with an adenovirus produced by a packaging cell line, wherein the adenovirus comprises an adenoviral vector comprising a promoter operably linked to a nucleic acid encoding the A subunit of diphtheria toxin (DT-A) or Pseudomonas Exotoxin A (PEA), and wherein the cell line is capable of producing adenovirus that expresses the A subunit of diphtheria toxin (DT-A) or Pseudomonas Exotoxin A (PEA), wherein the cell line does not produce replication-competent adenovirus when used in conjunction with non-overlapping E1-deleted adenovirus, wherein the cell line is resistant to DTA and PEA and wherein the cell line has a mutated human EF-2 gene that encodes an EF-2 protein that is mutated at codon 705. (Claim 16).

The Examiner argues that "the invention lies in the field of gene therapy (and) at the time the application was filed, gene therapy was considered to be unpredictable due to significant problems in several areas." (Office Action, p.3). The Examiner supports his argument regarding the state of gene therapy with a 1998 reference (Anderson et al. Nature Vol. 392), published **seven years prior to the 2005 filing date of the present application**. Nevertheless, the Examiner contends that the Anderson reference discusses issues surrounding gene therapy that include: 1) the type of vector and amount of DNA constructs;

2) the route and site of administration; 3) trafficking of genetic material, rate of degradation of the DNA, level and stability of mTNA; 4) therapeutically effective amount of expressed protein. (Office Action, p.3). The Examiner points out that Anderson et al. teaches that "gene therapy is a powerful new technology that still requires several years before it will make a noticeable impact on the treatment of disease." (Office Action, p.4). Given that Anderson is characterizing the state of the art prior to its publication in 1998, and given the more recent data and reports as cited herein demonstrating the successes of gene therapy in vivo at the time of filing, gene therapy has already made an impact on the treatment of disease.

In further support of the contention that the claims are not enabled, the Examiner cites the Verma et al., McNeish et al. and Vile et al. references, allegedly disclosing problems with gene therapy. These references describe general concepts regarding gene therapy, and are not current with the state of the art at the time of filing of the application. In this regard, to date there are dozens of clinical trials in the U.S., and many more around the world, that involve the use of gene therapy.

As described in the previous Office Action, a number of references demonstrate that administration of adenoviral therapeutics was known by those of skill in the art at the time the instant application was filed. Specifically, the work of Maria Castro et al. has demonstrated intracranial adenoviral delivery of Pseudomonas Exotoxin (PE) in an in vivo model. It is noted that Psuedomonas Exotoxin has the same catalytic activity as Diphtheria toxin, the difference being that one toxin has the catalytic subunit at the amino terminus and the other at the carboxy terminus. However, both Pseudomonas Exotoxin and Diptheria toxin cause ADP ribosylation at the diphtherimde residue in EF-2. Castro et al. demonstrate that adenoviral-mediated delivery of Pseudomonas Exotoxin (PE) Fused to IL-13 induces regression of intracranial human glioblastoma xenografts in mice (a copy of the abstract presented at the American Society for Gene Therapy 10th Annual Meeting is enclosed herewith (Seattle, WA. Simultaneous Oral Abstract Sessions: Cancer Gene Therapy (10:15 AM-12:15 PM), Saturday June 2, 2007), previously submitted).

Therefore, contrary to the Examiner's assertion, the methods of the present invention are enabled for methods of delivering the adenovirus as described herein.

As pointed out in the previous response, gene therapy has been used to treat severe combined immunodeficiency, for example, as taught by Blaese et al. (Science 270:475-480 (1995), where two children with a genetic defect in production of adenosine deaminase (ADA) were treated with a cloned ADA gene inserted into a retroviral vector. To this day both patients continue to display significant improvement in their immune system function. The results of this gene therapy treatment were markedly superior to those produced earlier by alternative treatment means. Further, Roth et al. (Nature Medicine 2(9):985-991 (1996)) have shown that a recombinant retroviral vector targets tumor cells in vivo. Moreover, this vector, which encodes the tumor suppressor p53, provided a sufficient level of p53 expression such that apoptosis, or programmed cell death, was triggered in these cells. Khuri et al. (Nature Medicine 6(8):879-885 (2000)) reported a successful gene therapy regimen in human cancer patients using ONYX-015, an oncolytic, chimeric group C adenovirus having a large deletion in the E1B gene. As previously pointed out, Cavazzana-Calvo et al. (Science 288:669-672 (2000)), have demonstrated full correction of disease phenotype in patients treated by gene therapy protocols. Further, Kay et al. (Nature Genetics 24:257-261 (2000)) have demonstrated therapeutic efficacy in the treatment of Haemophilia B with AAV vectors carrying the gene that encodes factor IX.

As pointed out in the prior response, even in a 1995 review article (Crystal, Science 270:404, 405 (1995)), the authors pointed out that human trials have show that "human gene transfer is indeed feasible...(and) genes can be transferred to humans whether the strategy is ex vivo or in vivo, and that all vector types function as intended."

Clearly, there is evidence to support successful human gene transfer in both ex vivo and in vivo studies.

Moreover, Applicants submit that the art available at the time the invention was made clearly shows that in vivo targeting for gene therapy was possible and effective at the time of filing of the present application.

For example, Yu et al. (Cancer Research 59:4200–4203 (September 1, 1999)), a copy of which is submitted herewith, construct CV787, a novel highly prostate-specific replication-competent adenovirus with improved efficacy. The CV787 adenovirus contains the prostate specific rat probasin promoter, driving the adenovirus type 5 (Ad5) E1A gene, and the human prostate-specific enhancer/promoter, driving the E1B gene, and the entire

Ad5 E3 region. Yu et al. report that when the CV787 adenovirus is injected in nu/nu mice carrying subcutaneous prostate cancer cell xenografts, a single intravenous. tail vein injection of CV787 eliminates tumors that are 300 mm^3 in size within 4 weeks. Thus, the adenovirus can be constructed to be prostate specific, and successfully targeted to kill target prostate cells in vivo.

In another example demonstrating that in vivo targeting was successfully used prior to the time of filing of the present application, Muzykantov et al. (Pharmacology 279(2): 1026-1034 (November 1, 1996)) use a new approach to deliver plasminogen activators to the luminal surface of the pulmonary vasculature in an effort to improve dissolution of pulmonary thromboemboli. A copy of Muzykantov et al. is enclosed herewith. Muzykantov et al. report the coupling of 125I-labeled biotinylated plasminogen activators to biotinylated mAb 9B9, using streptavidin as a cross-linker. Muzykantov et al. report that one hour after intravenous injection of mAb 9B9-conjugated radiolabeled biotinylated single-chain urokinase plasminogen activator, biotinylated tissue-type plasminogen activator or biotinylated-streptokinase in rats, the level of radiolabel was increased in the lung, compared to injection with control IgG. Thus, they show specific targeting to and prolonged association with the pulmonary vasculature, and another example of in vivo targeting for gene therapy.

In still another example demonstrating the success of in vivo targeting in gene therapy, Hicke et al. (J. Clin. Invest. 106(8): 923-928 (October 15, 2000)), a copy of which is enclosed herewith, describe the use of "escort aptamers" as targeting agents for in vivo diagnosis and therapy. The Hicke reference teaches that escort aptamers are designed to target radionuclides, toxins, or cytotoxic agents to diseased tissue, for example, the delivery of benign radionuclides for in vivo diagnosis of disease.

The Examiner alleges further that "it would take one skilled in the art an undue amount of experimentation to determine what route of administration...other than direct administration and/or systemic administration would result in a therapeutic response using a vector embraced in the claims." (Office Action, p.6). The Examiner argues further that "the applicants teach IJ or IP were suitable administration routes for delivering an adenovirus comprising the claimed nucleic acid into the liver of mice infected with HCV (but) the skilled artisan cannot reasonably extrapolate from the results using an adenovirus to a genus of vectors because each vector has a different mechanism and tropism." (Office Action, p.6

- 7). The Examiner alleges that "the instant specification and claims coupled with the art of record...only provide enablement for an in vitro method of suppressing growth of a cancer cell and an in vivo method of suppressing growth of a cancer cell in a subject comprising direct administration to the cancer cell and not for the full scope of the claimed invention." (Office Action, p.6).

For enablement purposes, a specification need not teach what is well known in the art. In re Wands, 858 F.2d 731 (Fed. Cir. 1988). Moreover, the need for some amount of experimentation is not fatal as long as the amount is not undue. Id. For the instant claims, no experimentation is required, because the specification provides sufficient guidance to allow one having ordinary skill in the art to make and use an adenovirus produced by a packaging cell line, wherein the cell line is capable of producing adenovirus that expresses the A subunit of diphtheria toxin (DT-A) or Pseudomonas Exotoxin A (PEA), wherein the cell line does not produce replication-competent adenovirus when used in conjunction with non-overlapping E1-deleted adenovirus, and wherein the cell line is resistant to DTA and PEA and wherein the cell line has a mutated human EF-2 gene that encodes an EF-2 protein that is mutated at codon 705 according to the claimed methods. More specifically, the disclosure details how to make DT resistant cells (e.g., p.11, line 20; p.12 - 13, example 1). Moreover, methods for the production of adenovirus using packaging cells as used in the methods of the invention are known in the art, as pointed out on page 9, line 14 of the disclosure.

Applicant submits that there is no requirement that Applicant provide data for every therapeutic method (see Amgen v. Chugai and Genetics Institute, 927 F.2d 1200 (Fed. Cir. 1991)). It is well established that examples are not required for an enabling disclosure. In re Robins, 166 U.S.P.Q. 552 (C.C.P.A. 1970); In re Borkowski, 164 U.S.P.Q. 642 (C.C.P.A. 1970). The first paragraph of 35 U.S.C. § 112 requires nothing more than objective enablement, which Applicant has provided. Thus, the examples included in the present application should be considered as supportive of enablement.

It is also respectfully submitted that a person having ordinary skill in the art, can take the adenovirus produced by the methods of the invention as set forth in the disclosure for administration to a subject by any method well known in the art, provided that they are amenable to the administration of adenovirus.

Accordingly, given the teaching in the art and the arguments presented above, Applicants submit that the claims are enabled as written. Applicants respectfully request that the Examiner withdrawn the foregoing rejection.

The Examiner has rejected claims 35 - 38 under 35 USC 112, second paragraph as allegedly being incomplete for omitting essential elements, such omission amounting to a gap between the elements. The Examiner argues that "(t)he omitted elements are: an adenoviral vector comprising a promoter operably linked to a nucleic acid encoding DT-A or PEA (and) while the claims define a cell line capable of producing the adenoviral vector, the claims do not include the adenoviral vector to complete the preamble of the claims." (Office Action, p.11). Applicants respectfully disagree.

While in no way acquiescing to the validity of the Examiner's rejection, and solely in the interest of advancing prosecution, Applicants have amended the claims to recite that the adenovirus comprises an adenoviral vector comprising a promoter operably linked to a nucleic acid encoding the A subunit of diphtheria toxin (DT-A) or Pseudomonas Exotoxin A (PEA).

Applicants respectfully request that the Examiner withdraw the foregoing rejection.

Docket No.: 58799(71699)

CONCLUSION

Applicants believe that the present application is now in condition for allowance. Favorable reconsideration of the application as amended is respectfully requested.

Applicants submit herewith a petition for a one month extension of time.

The Examiner is invited to contact the undersigned by telephone if it is felt that a telephone interview would advance the prosecution of the present application.

Dated: March 12, 2009

Respectfully submitted,

Jonathan M. Sparks

Registration No.: 53,624
EDWARDS ANGELL PALMER & DODGE LLP
P.O. Box 55874
Boston, Massachusetts 02205
(617) 439-4444
Attorneys/Agents For Applicant

PERSPECTIVE SERIES

Nucleic acid therapeutics
Bruce A. Sullenger, Series Editor

Escort aptamers: a delivery service for diagnosis and therapy

Brian J. Hicke and Andrew W. Stephens
Gilead Sciences, Boulder, Colorado, USA

Address correspondence to: Brian J. Hicke, Gilead Sciences, 2860 Wilderness Place, Boulder, Colorado 80301, USA.
Phone: (303) 546-7748; Fax: (303) 444-0672; E-mail: bhicke@gilead.com.

In 1990, the discovery of aptamers by Tuerk and Gold (1) and subsequently by Ellington and Szostak (2) spawned significant interest within academia and industry. Aptamers have quickly become valuable research tools (3–5). More than that, a therapeutic aptamer (6) has entered clinical evaluation just eight years after the inception of the technology. While aptamers have built inroads into therapeutic applications, they may also become important in vitro diagnostic tools (7). Here, we discuss a new development: the use of "escort aptamers" as targeting agents for in vivo diagnosis and therapy. Instead of directly interrupting a disease process, as would a function-blocking aptamer, escort aptamers are designed to deliver radionuclides, toxins, or cytotoxic agents to diseased tissue. Specifically, we focus on the delivery of benign radionuclides for in vivo diagnosis of disease. For discussion of function-blocking aptamers, see White et al., this Perspective series (8).

Aptamers and antibodies

The advent of monoclonal antibodies in 1974 brought to mind Paul Ehrlich's turn-of-the-century insight that molecules could serve as "magic bullets" that home to pathological organisms with precision (http://nobel.sdsc.edu/medicine/laureates/1908/ehrlich-bio.html). Indeed, the high affinity and specificity of antibodies provide some of the key properties in Ehrlich's concept. Despite some successes in tissue targeting, antibodies are saddled with a fundamental disadvantage: their large size (~155 kDa) results in slow tissue penetration and long blood residence. For example, in clinical settings where an antibody is coupled to a cell-killing radionuclide, this long circulation half-life leads to bone marrow toxicity that limits the permissible dose (9). To decrease blood half-life while maintaining target specificity, a second generation of smaller antibody fragments has been designed (10, 11). Antibody pretargeting strategies also show promise (12–14), and small peptides can have excellent pharmacokinetic profiles (15). However, many approaches are limited by complexity of clinical protocols, paucity of available targeting molecules, low-affinity binding, or immune responses by patients that prevent repetitive treatment cycles.

Because aptamers may provide solutions to many of these problems, they represent a promising new class of targeting agents. Having high affinity and specificity, and being synthetic polymers, aptamers combine the advantages of antibodies and small peptides in tissue targeting. To date, aptamers have not shown toxicity or immunogenicity following testing in several mammalian species (D. Drolet and R. Bendele, personal communication), suggesting that repeat dosing is possible in clinical settings. Finally, during the genomic/proteomic age, rapid discovery and development of high-affinity binding agents, as is possible with aptamer technology, will likely be advantageous in keeping pace with discoveries (16).

What is an aptamer?

Aptamers are modified oligonucleotides that are isolated by the systematic evolution of ligands by exponential enrichment (SELEX) process. Formally, aptamers are similar in composition to natural nucleic acids but are built with 2′-modified sugars to enhance resistance to blood and tissue nucleases. Aptamers are not linear molecules that carry genetic information. Rather, they are globular molecules, as exemplified by the shape of tRNA. Like antibodies, aptamers most frequently function through high-affinity binding to a target protein. This distinguishes aptamers from antisense oligonucleotides and ribozymes, which are designed to interrupt the translation of genetic information from mRNAs into proteins. At 8–15 kDa, escort aptamers are intermediate in size between small peptides (~1 kDa) and single-chain antibody fragments (scFv's; ~25 kDa).

Chemical synthesis, an advantage over proteins that aptamers share with small peptides (15), enables a wide range of site-specific modifications. This allows for engineering of an escort aptamer toward a specific purpose. For research, aptamers are readily tagged with fluorescent dyes, radionuclides, or biotin. For clinical purposes, escort aptamers can be conjugated to a variety of molecules, such as radionuclides or cytotoxic agents.

A notable example of aptamer plasticity was reported by Smith and colleagues (17), who used a modified SELEX process to blend high-affinity binding with covalent inhibition of an enzyme. To achieve enzyme inactivation, Smith and colleagues linked a weakly reactive valyl phosphonate moiety to a random aptamer pool, and selected for aptamers capable of rapid covalent linkage to human neutrophil elastase. The result is a combination of high-affinity binding with specific active-site inhibition. This pairing inactivates elastase nearly 100-fold more rapidly than do peptide-based phosphonate inhibitors. This aptamer has been further modified to incorporate a radio-metal chelation moiety and has been used to target neutrophil-bound elastase in an in vivo inflammation model (17).

Many aptamer adaptations use simple succinimidyl ester chemistry, which is accessible even to the most faint-of-heart among us. Importantly, modification can be directed to a single site away from the aptamer's active surface, preventing loss of function. Radiolabeling and conjugations can be performed using high temperatures (95°C), organic solvents, and pH ranging from 4 to 8.5. Thus, escort aptamers can attend a variety of functions through their chemical adaptability.

Aptamer isolation: the SELEX process

The SELEX process at the heart of aptamer isolation consists of iterative steps of binding and amplification using a combinatorial library of oligonucleotides (see White et al., this Perspective series, ref. 8; and ref. 18). In this respect, it is fundamentally similar to phage display (19) and ribosome display (20) technologies that are used for generation of antibody fragments and peptides. Before beginning the SELEX process, a single-stranded DNA oligonucleotide pool must be chemically synthesized with fixed sequences at either end, flanking a region of (typically) 40 randomized nucleotides. From this theoretical maximum "sequence space" of 10^{24} distinct nucleotide sequences, about 1 nmol, corresponding to about 10^{15} sequences, is used as a template for generating a 70-nucleotide transcript with RNA polymerase. To initiate the SELEX process, the oligonucleotide pool is incubated with the target protein. Aptamers bound to the protein are partitioned away from unbound oligonucleotides and then amplified and transcribed to close one round of the process. Subsequent selection rounds further cull the pool, as pressure is applied to yield only high-affinity interactions. Typically, five to eight rounds are required for completion, which is usually defined by a plateau in affinity for the target protein. These steps are automatable (21, 22), which implies that the SELEX process can keep pace with accelerating target discovery rates.

To diversify aptamer libraries, 5-position adducts on pyrimidines can be blended into the SELEX process. As an example, introduction of benzyl and pyridyl moieties allows for presentation of increased hydrophobicity to target proteins that are less likely to find polyanionic oligonucleotides attractive. Protein-like functionality can also be incorporated: primary amine, carboxylic acid, and imidazole side chains increase the chemical diversity of aptamer libraries (23). In addition, the SELEX process can be adapted to identify aptamers that interact with their targets in a covalent manner. For example, the pyrimidine 5-position is available for attachment of chemically and photochemically reactive moieties. The adducts chosen for this purpose are generally weakly reactive except in the context of an appropriate aptamer, so undesirable crosslinking to nontarget serum proteins is rare, and covalent linkage is strictly dependent on formation of a specific aptamer–protein complex.

At completion of the SELEX experiment, an aptamer pool is cloned and sequenced, and aptamers are screened for affinity. For the most efficient chemical synthesis, clones are truncated to the smallest size possible while retaining high affinity (Figure 1). Typically, such size-minimized aptamers range from 25 to 45 nucleotides in length.

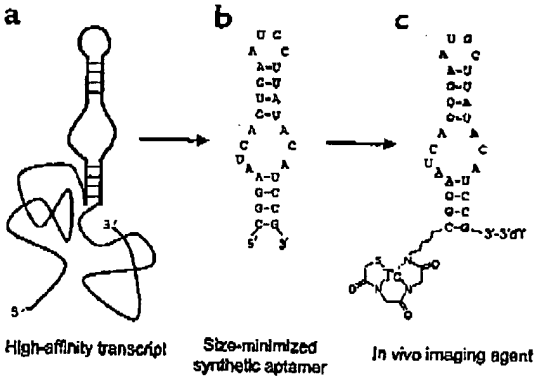

Figure 1
An archetypal escort aptamer. (a) A high-affinity aptamer is identified by the SELEX process. 2′-F pyrimidines are incorporated during selections. (b) The aptamer is truncated to minimal size and is now a synthetic molecule. (c) The escort aptamer as an in vivo diagnostic agent. Further nuclease stabilization is achieved: only two positions remain 2′-OH (underlined); the remainder are 2′-F pyrimidine and 2′-OCH_3 purine (bold). Chemical synthesis adds a 3′-3′ exonuclease cap and a primary amine (or thiol, etc.) for desired modifications. For in vivo imaging, a radiometal chelator is conjugated to the 5′ amine and ^{99m}Tc is incorporated.

Engineering chemical stability

Early in the development of function-blocking aptamers, it was appreciated that the inherent instability of RNA and DNA in blood is a fundamental limitation to therapeutic utility. This observation led the antisense research community to develop nucle-

ase-resistant oligonucleotides with modified phosphate backbones, including phosphorothioate and methyl phosphonate linkages. However, such backbone modifications are not compatible with the enzymatic steps of the SELEX process, and this forces the development of alternative solutions to the nuclease cleavage problem.

During nuclease cleavage, the ribose 2′-OH engages in nucleophilic attack on the neighboring 3′ phosphodiester bond. Therefore, 2′ modifications that diminish reactivity can effect significant nuclease resistance in plasma (24). In contrast to backbone substitutions, many 2′ ribose modifications are compatible with the SELEX process enzymes. Further, unlike phosphorothioate oligonucleotides, 2′-modified aptamers maintain low binding to serum proteins, a feature that is critical in permitting escort aptamers to be targeted specifically to the tissue of interest. As a result of the modifications, RNAs containing 2′-F and 2′-NH_2 pyrimidines are at least 1,000-fold more resistant to degradation in plasma than their unmodified RNA counterparts (24).

Final steps in escort aptamer preparation involve synthetic modifications of the truncated aptamer. Further nuclease stabilization is achieved by substitution of 2′-OCH_3 for 2′-OH at purine positions. As the 2′-OCH_3 moiety is not compatible with current SELEX process enzymes, this alteration must occur during chemical synthesis following evolution of a specific aptamer sequence. Generally, most of the 2′-OH purines can be substituted without loss of binding activity. At some locations, purines cannot be substituted without loss of affinity. In addition to protection against endonucleases, it is useful to protect against 3′ exonuclease activity. Therefore the 3′ nucleotide is inverted to form a new 5′-OH, with a 3′-3′ linkage to the penultimate base. Finally, synthesis incorporates nucleophilic amines or thiols, lending flexibility for attachment of the escorted species or other desirable modifications.

An archetypal escort aptamer structure is shown in Figure 1c. It is a size-minimized oligonucleotide that exits the SELEX process and is truncated, further protected against nucleases, and conjugated to its payload. For in vivo imaging, we typically couple a radiometal chelator to the 5′ terminus. In the example shown, the chelator (25) incorporates the metastable isotope technetium-99m (^{99m}Tc), an isotope commonly used in clinical settings.

Aptamers as targeting agents

At least six properties can be ascribed to the ideal targeting agent: high affinity and specificity for the target molecule, rapid uptake in the target tissue, rapid blood clearance, urinary excretion, durable tissue retention, and accumulation of high concentrations in the target tissue. The efficacy of a targeting agent is the aggregate of performance in each area. To interpret the strengths and weaknesses of escort aptamers in each category, we have initially focused on delivery of a benign radionuclide, ^{99m}Tc. Unless otherwise stated, pharmacokinetic parameters discussed here refer to the escorted ^{99m}Tc radiolabel, not to the aptamer per se.

Affinity and specificity are crucial for retention in the target tissue and low uptake in nontarget tissues. For antibodies, the relationship of affinity with uptake level in the target tissue is clear: within limits, increased affinity leads to greater uptake (26). Aptamers typically have high affinity for their target proteins, ranging from 0.05–10 nM, equilibrium dissociation constants that compare favorably with those of scFv's and are considerably better than those generally reported for peptides derived from phage display experiments. Tumor-targeting agents need to differentiate between normal and malignant forms of the same tissue, again requiring the specificity that aptamers generate (6). Affinity and specificity are not sufficient, however. Pharmacokinetic and tissue distribution characteristics are also critical and can doom an otherwise promising agent.

In comparing antibody fragments to antibodies (10), the transition from monomeric to multimeric forms leads to improved tumor uptake, but generally decreases tumor/blood ratios. At 15–30 kDa, a dimeric aptamer would have roughly equivalent mass to a monomeric scFv, ~25 kDa. In one case, dimerization of a function-blocking aptamer that binds to a cell surface protein results in a tenfold decrease in aptamer dissociation rate from lymphocytes (27). For escort aptamers, the effects of dimerization on tissue target-

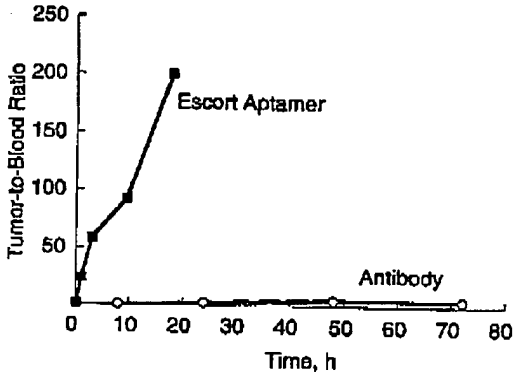

Figure 2
Tumor/blood ratios of escort aptamer and antibody. Radiolabeled aptamer and antibody against the same target protein were administered by intravenous bolus injection into tumor-bearing mice. Concentrations in the target tissue and blood were determined, and the target/blood concentration ratio was plotted against time. Because of differing distribution and clearance kinetics, different time points were chosen for aptamer and antibody.

ing are not yet known. Regardless of any changes made by increasing avidity, current escort aptamers have very high affinity and specificity.

Rapid image development is an increasingly important clinical parameter in targeting, in part because of the managed health care environment, which demands that diagnostic studies be performed quickly in an outpatient setting. Aptamers display rapid image development, as depicted graphically in Figure 2, which compares tumor targeting by an aptamer and an antibody that bind to the same protein. The antibody requires days to achieve an appreciable signal/noise ratio. In contrast, the aptamer rapidly develops a far higher signal/noise ratio that results in high-quality tumor images (B.J. Hicke, unpublished observation). The slow uptake and clearance of antibodies is due in part to their large size. While smaller antibody fragments show improvements relative to intact antibodies, peptides (15) and now escort aptamers have still more favorable kinetics, which fit well with anticipated clinical needs for in vivo imaging.

For in vivo imaging using ^{99m}Tc, signal/noise ratios are important parameters, and here we focus on a critical parameter, the target/blood ratio. After intravenous injection of two different ^{99m}Tc-radiolabeled aptamers, maximal levels are observed in either clots or tumors within 10–30 minutes. In addition to rapid tissue uptake, these escort aptamers display rapid clearance, as defined here by ^{99m}Tc removal from blood. For tumor- and clot-targeting escort aptamers, 99% of the blood ^{99m}Tc is cleared with a half-life of less than 5 minutes in the mouse. This desirable clearance rate is more comparable to small peptides than to scFv's or antibodies. At 8–15 kDa, escort aptamers are small enough to permit rapid renal filtration and rapid access to extravascular tissues (for function-blocking aptamers against intravascular proteins, longer blood residence is desirable and is obtained by conjugation to 40 kDa polyethylene glycol [28]). As nuclease cleavage occurs during the time scale of these measurements, ^{99m}Tc-labeled aptamer metabolites will also contribute to clearance. For in vivo imaging, current escort aptamer forms develop favorable target/blood ratios in animal models, primarily driven by rapid blood clearance rates.

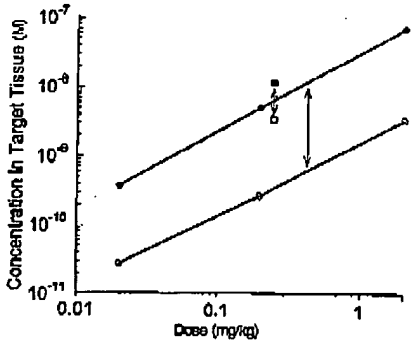

Figure 3
Comparison of tumor targeting by escort aptamer and antibody. ^{99m}Tc-radiolabeled aptamer and ^{125}I-radiolabeled antibody against the same target protein were administered by intravenous bolus injection into tumor-bearing mice. Concentration of aptamer was measured at 1 hour in tumor (filled circles) and blood (open circles), and concentration of antibody was measured at 24 hours in tumor (filled square) and blood (open square). Three doses of aptamer are compared with each other and with a single dose of antibody. Signal/noise ratios of antibody and aptamer at equivalent tumor loading are represented by the lengths of the double-headed arrows. Note: for both aptamer and antibody, the time of measurement was before optimal tumor/blood ratios were achieved (see Figure 2).

Another desired feature of the ideal targeting agent is urinary excretion, which tends to be much more rapid than hepatobiliary excretion. In mice, current escort aptamers produce approximately 60% urinary clearance of the injected ^{99m}Tc within 3 hours (in rabbits, urinary excretion proceeds to a greater extent). The remaining radioactivity (40%) is cleared through the hepatobiliary system. This is a disadvantage to current escort aptamer formulations, as radioactivity passing through the liver and intestines can obscure in vivo images of abdominal targets. It remains to be seen whether heparobiliary clearance is a clinically significant hurdle. For peptide targeting agents, the balance of urinary and hepatobiliary excretion can be readily altered by modification of the ^{99m}Tc chelating moiety (15), and this is also the case for escort aptamers in rodent studies.

An unexpected feature of aptamers is durable retention in the preferred tissue, with a half-life of more than 12 hours for a tumor-targeting aptamer in the mouse. While the reason for long retention has not been addressed, we were surprised to discover that tumor- and clot-associated escort aptamers remain mostly intact for hours, with some variation depending on the aptamer and the animal species. In contrast to target-bound aptamers, nuclease degradation of blood-borne aptamers occurs rapidly, with greater than 95% destruction within 30 minutes in blood. Currently, we feel that targeted, as opposed to blood-borne, escort aptamers are stable because the bulk of degradation occurs at sites (perhaps the liver and kidney) that are anatomically separate from the target tissue. Consistent with this model, we have noted that aptamer clearance from the blood is dramatically slower in hepatectomized rats (A.W. Stephens, unpublished observation). As an aside, the observed protection of target-bound aptamer from nucleases has implications for the development of function-blocking nucleic acids, including aptamers, antisense, and ribozymes, that operate in extravascular tissues: in optimizing pharmacokinetics, it may

become important to measure target tissue levels as well as blood residence time. Independent of the mechanism, durable target tissue residence is a primary factor in the high signal/noise ratios (as high as 50 within 3 hours) achieved with escort aptamers.

Finally, an ideal escort displays high uptake in the target tissue. High uptake increases the sensitivity of an imaging agent. Often, uptake of imaging agents is measured as percent of the injected dose per gram (% ID/g) of tissue. We have compared an escort aptamer with an antibody for the same target protein. When quantitated using the % ID/g method, the aptamer has 15-fold lower uptake than the antibody at an equivalent dose (data not shown). An alternative analysis measures molar concentration in the target tissue. Figure 3 compares antibody and aptamer in this way and reveals three principles. First, at an equivalent dose, molar uptake of the aptamer is reduced only twofold compared with the antibody. Second, to achieve equivalent tumor loading, one can simply increase the aptamer dose twofold. Third, at a comparable tumor loading level, denoted by the double-headed arrows in the figure, the aptamer displays much higher signal/noise ratios (20 at 1 hour after injection) than does the antibody (3.5 at 24 hours after injection). Like the escort aptamer, scFv's and high-affinity peptides have improved clearance rates but lower % ID/g than antibodies. The desired comparison between aptamer, scFv, and peptide has not yet been possible. To summarize, small increases in escort aptamer dose compensate for lower % ID/g tissue uptake compared with antibodies and fragments thereof, with retention of high signal/noise ratios.

Since all targeting molecules fall short in one or more of these six categories, there is as yet no magic bullet. As targeting agents, aptamers are currently described as having high-affinity binding and durable retention in target tissue, rapid tissue penetration and blood clearance, and both urinary and hepatobiliary clearance pathways. Experimental approaches to improvement include testing dimeric aptamer forms with increased avidity, exploring the effect of increases in nuclease stability, and chemical alterations to increase urinary clearance and decrease hepatobiliary clearance. In optimizing the properties of escort aptamers, it will be necessary to more thoroughly define clearance pathways and the effect of aptamer metabolism on tissue targeting. The ease of chemical synthesis and modification allows one to rapidly screen aptamer formulations for increased performance.

Radiotherapeutic applications of escort aptamers

While improved in vivo imaging would be valuable, escort aptamer characteristics also suggest utility in cancer therapy. The transition to therapy awaits clinical assessment of escort aptamers as imaging agents. Nevertheless, current preclinical work identifies some issues to be addressed for this transition. Hepatobiliary clearance, if observed clinically, is not favorable due to increased exposure of radiosensitive intestinal epithelia. Radioisotope choice can help alleviate concerns caused by hepatobiliary clearance. For example, α-particle radiotherapy is attractive for two reasons. First, a short half-life (46 minutes in the case of ^{213}Bi) decreases intestinal exposure because of decay during transit to the intestines. Second and more important, the α particle has a very short path length (<100 μM) relative to the intestinal lumen diameter, suggesting that a minute fraction of intestinal ^{213}Bi decay events will reach the radiosensitive epithelium. In terms of efficacy, the escort aptamer's tumor penetration rate exceeds the ^{213}Bi decay rate. Because escort aptamer pharmacokinetics match ^{213}Bi decay kinetics, a large increase in therapeutic index may be possible with an α particle–emitting aptamer as compared with an aptamer conjugated to the β-emitting isotope ^{90}Y. In fact, a preclinical radiotherapy comparison using a 50-kDa antibody fragment indicates that the α particle–emitting fragment has a far higher cure rate than the corresponding β particle–emitting antibody fragment (29).

Escort aptamers as a new class of targeting molecules

As oligonucleotide analogs of antibodies, escort aptamers are well tailored for delivering radionuclides to sites of diseased tissue. Significant work is needed to fully assess escort aptamer potential, but it appears that aptamers will be important targeting agents due to their high affinity, rapid blood clearance, and adaptability through organic synthesis. An aptamer can be rapidly identified and carried through discovery, optimization, and application to research and clinical problems.

In the near future, escort aptamers will need to be tested to determine how animal models translate into the clinic. Clinical behavior will provide important feedback to preclinical design in both imaging and therapy. While no single magic bullet will likely be found, the emergence of scFv's, antibody pretargeting strategies, and small peptides suggests that over the horizon lies an array of specific targeting agents. What will escort aptamers bring to the party?

Acknowledgments

Critical contributions came from many, including Philippe Bridonneau, Gary Cook, David Parma, Paul Schmidt, Drew Smith, and Steve Warren. Colleagues Ulrich Speck, Ludger Dinkelborg, and Stephan Hilger have supplied additional expertise. Martin Brechbiel and Brian Moyer provided helpful input on α-particle radiotherapy. Dan Drolet and Ray Bendele

made helpful additions to this manuscript. Finally, Larry Gold's commitment to aptamer research has made this work possible.

1. Tuerk, C., and Gold, L. 1990. Systematic Evolution of Ligands by EXponential enrichment: RNA ligands to bacteriophage T4 DNA polymerase. *Science.* 249:505–510.
2. Ellington, A.D., and Szostak, J.W. 1990. In vitro selection of RNA molecules that bind specific ligands. *Nature.* 346:818–822.
3. Gold, L. 1995. Oligonucleotides as research, diagnostic, and therapeutic agents. *J. Biol. Chem.* 270:13581–13584.
4. Famulok, M., and Mayer, G. 1999. Aptamers as tools in molecular biology and immunology. *Curr. Top. Microbiol. Immunol.* 243:123–136.
5. Gold, L., et al. 1995. Diversity of oligonucleotide functions. *Annu. Rev. Biochem.* 64:763–797.
6. Ruckman, J., et al. 1998. 2'-Fluoropyrimidine RNA-based aptamers to the 165-amino acid form of vascular endothelial growth factor (VEGF165). Inhibition of receptor binding and VEGF-induced vascular permeability through interactions requiring the exon 7-encoded domain. *J. Biol. Chem.* 273:20556–20567.
7. Jayasena, S.D. 1999. Aptamers: an emerging class of molecules that rival antibodies in diagnostics. *Clin. Chem.* 45:1628–1650.
8. White, R.R., Sullenger, B.A., and Rusconi, C.P. 2000. Developing aptamers into therapeutics. *J. Clin. Invest.* 106:929–934.
9. Knox, S.J., and Meredith, R.F. 2000. Clinical radioimmunotherapy. *Semin. Radiat. Oncol.* 10:73–93.
10. Adams, G.P., and Schier, R. 1999. Generating improved single-chain Fv molecules for tumor targeting. *J. Immunol. Methods.* 231:249–260.
11. Wu, A.M., et al. 1996. Tumor localization of anti-CEA single-chain Fvs: improved targeting by non-covalent dimers. *Immunotechnology.* 2:21–36.
12. Boerman, O.C., et al. 1999. Pretargeting of renal cell carcinoma: improved tumor targeting with a bivalent chelate. *Cancer Res.* 59:4400–4405.
13. Paganelli, G., et al. 1999. Antibody-guided three-step therapy for high grade glioma with yttrium-90 biotin. *Eur. J. Nucl. Med.* 26:348–357.
14. Axworthy, D.B., et al. 2000. Cure of human carcinoma xenografts by a single dose of pretargeted yttrium-90 with negligible toxicity. *Proc. Natl. Acad. Sci. USA.* 97:1802–1807.
15. Lister-James, J., Moyer, B.R., and Dean, T. 1996. Small peptides radiolabeled with 99mTc. *Q. J. Nucl. Med.* 40:221–233.
16. Gold, L., and Alper, J. 1997. Keeping pace with genomics through combinatorial chemistry. *Nat. Biotechnol.* 15:297.
17. Charlton, J., Sennello, J., and Smith, D. 1997. In vivo imaging of inflammation using an aptamer inhibitor of human neutrophil elastase. *Chem. Biol.* 4:809–816.
18. Fitzwater, T., and Polisky, B. 1996. A SELEX primer. *Methods Enzymol.* 267:275–301.
19. Winter, G., et al. 1994. Making antibodies by phage display technology. *Annu. Rev. Immunol.* 12:433–455.
20. Hanes, J., and Pluckthun, A. 1997. In vitro selection and evolution of functional proteins by using ribosome display. *Proc. Natl. Acad. Sci. USA.* 94:4937–4942.
21. Drolet, D.W., et al. 1999. A high throughput platform for systematic evolution of ligands by exponential enrichment (SELEX). *Comb. Chem. High Throughput Screen.* 3:271–278.
22. Cox, J.C., Rudolph, P., and Ellington, A.D. 1998. Automated RNA selection. *Biotechnol. Prog.* 14:845–850.
23. Eaton, B.E. 1997. The joys of in vitro selection: chemically dressing oligonucleotides to satiate protein targets. *Curr. Opin. Chem. Biol.* 1:10–16.
24. Picken, W.A., et al. 1991. Kinetic characterization of ribonuclease-resistant 2'-modified hammerhead ribozymes. *Science.* 253:314–317.
25. Hilger, C.S., et al. 1999. Tc-99m-labeling of modified RNA. *Nucleosides Nucleotides.* 18:1479–1481.
26. Adams, G.P., et al. 1998. Increased affinity leads to improved selective tumor delivery of single-chain Fv antibodies. *Cancer Res.* 58:485–490.
27. Ringquist, S., and Parma, D. 1998. Anti-L-selectin oligonucleotide ligands recognize CD62L-positive leukocytes: binding affinity and specificity of univalent and bivalent ligands. *Cytometry.* 33:394–405.
28. Watson, S.R., et al. 2000. Anti-L-selectin aptamers: binding characteristics, pharmacokinetic parameters, and activity against an intravascular target in vivo. *Antisense Nucleic Acid Drug Dev.* 10:63–75.
29. Behr, T.M., et al. 1999. High-linear energy transfer (LET) alpha versus low-LET beta emitters in radioimmunotherapy of solid tumors: therapeutic efficacy and dose-limiting toxicity of 213Bi- versus 90Y-labeled CO17-1A Fab' fragments in a human colonic cancer model. *Cancer Res.* 59:2635–2643.

[CANCER RESEARCH 59, 4200–4203, September 1, 1999]

Advances in Brief

The Addition of Adenovirus Type 5 Region E3 Enables Calydon Virus 787 to Eliminate Distant Prostate Tumor Xenografts

De-Chao Yu, Yu Chen, Monica Seng, Jeanette Dilley, and Daniel R. Henderson[1]

Calydon, Inc., Sunnyvale, California 94089

Abstract

CV787, a novel highly prostate-specific replication-competent adenovirus with improved efficacy, was constructed. CV787 contains the prostate-specific rat probasin promoter, driving the adenovirus type 5 (Ad5) *E1A* gene, and the human prostate-specific enhancer/promoter, driving the *E1B* gene. To improve efficacy, we constructed CV787 such that it also contains the entire Ad5 E3 region. CV787 replicates in prostate-specific antigen (PSA)$^+$ cells as well as wild-type adenovirus, but in PSA$^-$ cells, CV787 replicates 10^4–10^5 times less efficiently. CV787 destroys PSA$^+$ prostate cancer cells 10,000 times more efficiently than PSA$^-$ cells. Incorporation of the Ad5 E3 region significantly improves the target cell killing ability or efficacy of CV787. In *nu/nu* mice carrying s.c. LNCaP xenografts, a single i.v. tail vein injection of CV787 eliminates 300-mm^3 tumors within 4 weeks. CV787 could be a powerful therapeutic for human metastatic prostate cancer.

Introduction

Prostatic cancer is the second leading cause of cancer-related deaths in men in the United States (39,000 deaths in 1998; Ref. 1). Current treatment for metastatic prostate cancer is androgen ablation therapy, which, in 70% of men, provides relief from otherwise uncontrollable bone pain and increases life expectancy by 6–18 months. Clearly, a new approach to metastatic prostate cancer treatment is needed (2–4).

We previously constructed a prostate-specific ARCA,[2] CN706, in which the Ad5 *E1A* gene is driven by PSE (5, 6). CN706 destroys human PSA$^+$ cells 400 times more efficiently than PSA$^-$ cells and eliminates LNCaP xenografts in *nu/nu* mice with a single i.t. injection. To improve the specificity of CN706, we placed both the Ad5 *E1A* and *E1B* genes under the control of prostate-specific transcriptional regulatory elements. CV764 contains the PSE, driving the Ad5 *E1A* gene, and the promoter/enhancer of a second human prostate-specific gene, the *hKLK2* gene, driving the Ad5 *E1B* gene. CV764 destroys PSA$^+$ cells 10,000 times more efficiently than PSA$^-$ cells and cannot productively infect PSA$^-$ cells (7). However, CN706 and CV764 could not eliminate distant preexistent LNCaP xenograft tumors in *nu/nu* mice by i.v. tail vein administration (data not shown).

To improve efficacy by systemic i.v. administration, we, led by preliminary evidence (data not shown), restored the Ad5 E3 region (nucleotides 28133–30818). The E3 region had been deleted in both CN706 and CV764 (6–8). The E3 region has long been considered unnecessary for replication of adenovirus *in vitro* and has been universally deleted from Ad5 gene therapy constructs until recent efforts to reduce the immune response to the vector (9–14). The Ad5 E3 region encodes proteins that play a role in assisting virus release and evading or slowing host immune responses to the virus (15–25). CV764 did not have the genome space required to include the entire E3 region, but we wished to retain the specificity of using two independent prostate-specific transcriptional regulatory elements driving the Ad5 *E1A* and *E1B* genes. Thus, we constructed CV787 using the rat probasin prostate-specific promoter (26–28), driving the *E1A* gene, and the PSE, driving the *E1B* gene, and retained the entire Ad5 E3 region. The CV787 genome length is 105% the length of wt Ad5, yet the virus replicates well and is completely stable. CV787 is an ARCA that replicates like wt Ad5 in cells that express PSA but is attenuated 10,000–100,000 times, with respect to replication in PSA$^-$ cells. CV787 is highly cytopathogenic in PSA$^+$ cells and is capable of eliminating distantly located preexisting prostate tumors following i.v. injection.

Materials and Methods

Virus Constructions. CV787 was constructed by insertion of the rat probasin promoter and the human PSE, driving the Ad5 *E1A* and *E1B* genes, respectively. pXC1, pBHG10, and pBHGE3 were purchased from Microbix Biosystems (Ontario, Canada; Refs. 8 and 29). pXC1 contains the Ad5 bp 22–5790, including the inverted terminal repeat, the packaging sequence, and the *E1A* and *E1B* genes inserted into pBR322 (29). pBHGE3 contains the entire Ad5 genome, except for a deletion between Ad5 bp 188 and 1339, inserted into pBR322 (8). pBHG10 is similar to pBHGE3, except that it is E3 deleted (ΔAd5, nucleotides 28133–30818). pXC1 was modified to contain an *AgeI* site at bp 547 between the E1A mRNA cap site and the E1A translation initiation site by inserting a T between Ad5 bp 551 and 552, yielding CP95 (6). CP95 was modified to create an *EagI* site at Ad5 bp 1681 between the E1B promoter and the E1B mRNA cap site. The *EagI* site was created by inserting a G between Ad5 bp 1681 and 1682 into CP95 using overlap PCR with the following two sets of primers. The first set (primer i, 5′-TCGTCTTCAA-GAATTCTC-3′; and primer ii, 5′-GCCCA*CGGCCG*CATTATATAC-3′; *EagI* site is italicized), amplifies a 2090-bp fragment in CP95, and the second set (primer iii, 5′-GTATATAATG*CGGCCG*TGGGC-3′; and primer iv, 5′-CCAGAAAATCCAGCAGGTACC-3′), amplifies a 399-bp fragment from the same plasmid. The two PCR products were annealed in equal molar ratios and used as template for PCR with primers i and iv. The 2468-bp overlap product was digested with *EcoRI* and *KpnI* and ligated to similarly cut CP95, creating CP124. CP125 was constructed by cloning the PSA 5′-flanking sequence, containing the enhancer domain from −5322 to −3875 from the transcription start site and the promoter from −230 to +7, into the *EagI* site of CP124 (6). CP257 was constructed by cloning the rat probasin promoter (positions −426 to +28; Ref. 26) into the *AgeI* site of CP125. The rat probasin promoter was amplified by PCR from rat genomic DNA (Clontech, Palo Alto, CA) with primers (5′-GATC*ACCGGT*AAGCTTCCACAAGTGCATTTAGCC-3′ and 5′-GATC*ACCGGT*CTGTAGGTATCTGGACCTCACTG-3′) containing *AgeI* sites (italicized). The PCR product was digested with *PinAI* (an isoschizomer of *AgeI*) and cloned into a similarly cut CP125, creating CP257. CV739, CV787, and CV802 were generated by homologous recombinations of CP257 and pBHG10, CP257 and pBHGE3, and pXC1 and pBHGE3, respectively (8, 10, 30). Fig. 1 shows the structures of CN702, CN706, CV739, CV787, and CV802. Viruses were grown and purified as described previously (6, 7). The particle:pfu ratio of all viruses was 20:1.

Received 4/21/99; accepted 7/20/99.

The costs of publication of this article were defrayed in part by the payment of page charges. This article must therefore be hereby marked *advertisement* in accordance with 18 U.S.C. Section 1734 solely to indicate this fact.

[1] To whom requests for reprints should be addressed, at Calydon Inc., 1324 Chesapeake Terrace, Sunnyvale, CA 94089. Phone: (408) 734-0733; Fax: (408) 734-2808; E-mail: dhenderson@calydon.com.

[2] The abbreviations used are: ARCA, attenuated replication-competent adenovirus; Ad5, adenovirus type 5; P, virus particle; PSA, prostate-specific antigen; PSE, PSA promoter and enhancer; i.t., intratumoral(ly); wt, wild-type; pfu, plaque-forming unit(s); MTT, 3-[4,5-dimethylthiazole-2–4]-2,5-diphenyl-2H-tetrazolium bromide.

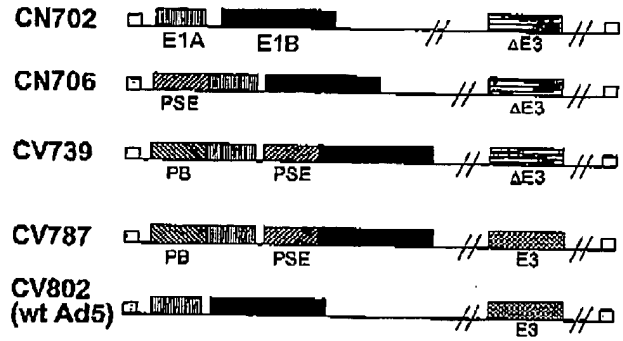

Fig. 1. Structure of viruses. CN706 contains the PSE, driving the Ad5 *E1A* gene, but is Ad5 E3 region deleted; CV739 contains the rat probasin promoter, driving the Ad5 *E1A* gene, and the PSE, driving the Ad5 *E1B* gene, but is Ad5 E3 region deleted; CV787 is identical to CV739 but contains the Ad5 E3 region; and CV802 is a constructed wt Ad5 containing a normal Ad5 E1 region and a normal Ad5 E3 region.

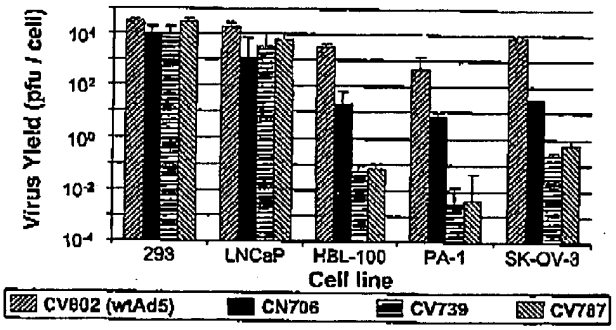

Fig. 2. Burst sizes of CN706, CV739, CV787, and CV802 (wt Ad5) in PSA$^+$ and PSA$^-$ cells. Cells were infected at a multiplicity of infection of 2, virus was harvested 48 h after infection, and virus yield was determined by plaque assay on 293 cells.

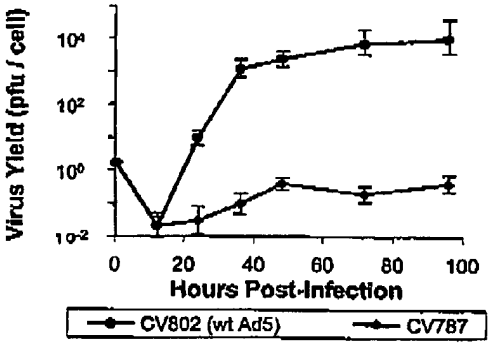

Fig. 3. Growth curves of CV787 and CV802 (wt Ad5) in hMVEC cells. Cells were infected at a multiplicity of infection of 2, virus was harvested at indicated times after infection, and virus yield was determined by plaque assay on 293 cells.

Cell Culture. Cells were obtained and maintained as described previously (6, 7). Plaque assays were determined as described previously (6, 7). Burst sizes of CN706, CV739, CV787, and CV802 (wt Ad5) in PSA$^+$ and PSA$^-$ cells were determined as follows. Cell monolayers (2×10^5 cells/well) in six-well plates were inoculated with 4×10^5 pfu of CN706, CV739, CV787, or CV802 (wt Ad5; Refs. 7 and 8). Virus yields were titrated at 48 h after infection. Cells were infected in duplicate; assays were carried out in triplicate.

One-step growth curves of CV787 and CV802 (wt Ad5) were performed in human microvascular endothelial cell (hMVEC) monolayers. Monolayers of hMVEC cells were infected at a multiplicity of 2 pfu/cell with either CV787 or CV802 (wt Ad5). At the indicated times thereafter, duplicate cell samples were harvested and lysed by three cycles of freeze-thawing, and the virus in the supernatants was assayed in triplicate in 293 cell monolayers. One-step growth curves of CV787 in LNCaP cells using medium containing charcoal-stripped serum with or without R1881 (methyltrienolone) were performed similarly. Cytopathogenity of CV787 and CV802 (wt Ad5) was also determined in hMVEC monolayers, as described previously (7)

Cell survival of PSA$^+$ and PSA$^-$ cells infected with either CV787 or CV802 (wt Ad5) was determined. Monolayers of LNCaP, HBL-100, and OVCAR-3 cells were infected at a multiplicity of 1 pfu/cell with either CV787 or CV802 (Ad5). Cell survival (viability) comparing the effect of the E3 region with CV739 and CV787 in LNCaP cells was assessed by measuring mitochondrial activity using MTT (17).

***In Vivo* Animal Experiments.** LNCaP xenograft tumors in *nu/nu* were induced in 6–7-week-old BALB/c *nu/nu* mice and allowed to grow to an average volume of 300 mm^3 (6). Fifty μl of CV787 in PBS-10% glycerol or PBS-10% glycerol alone were injected into the tail vein. Tumor size was measured weekly, as described previously (6). Serum samples were collected by tail vein incision. PSA levels were measured using an immunoassay kit (Genzyme Diagnostics, San Carlos, CA).

Results and Discussion

Specificity of CV787. The target cell specificity of CV787, relative to that of wt Ad5, was tested in Ad5 E1A$^+$ and E1B$^+$ 293 cells, PSA$^+$ human LNCaP prostate cells, and a panel of PSA$^-$ cells, including human breast epithelial HBL-100 cells, ovarian cancer OVCAR-3 cells, and PA-1 cells. Fig. 2 shows the 48-h burst sizes of CN706, CV739, CV787, and CV802 (wt Ad5). The burst size of CV802 (wt Ad5) in these cells ranged from 3×10^3 to 2×10^4, and

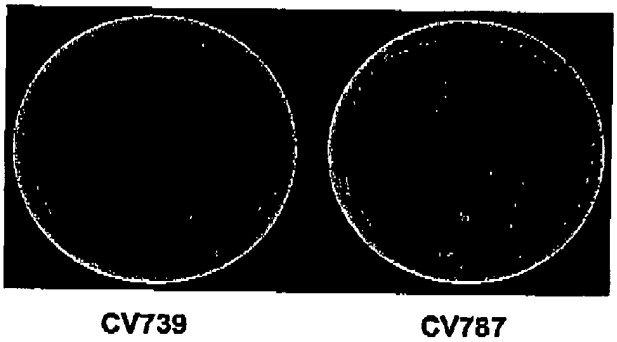

Fig. 4. Plaque morphology of CV739 and CV787. 293 cells were infected with CV739 and CV787. After a 4-h adsorption period, plates were overlayed with agar and incubated for 10 days. After 10 days, the agar overlay was removed, and the cells were stained with crystal violet.

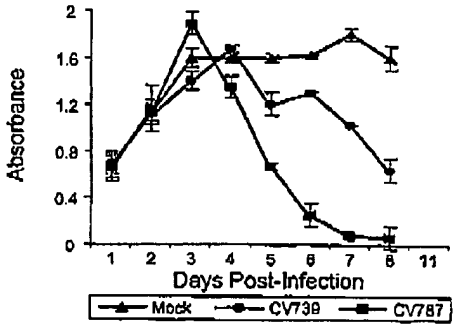

Fig. 5. Comparison of CV739 and CV787 on mitochondrial activity of infected LNCaP cells. Cells were infected with CV739 and CV787 at a multiplicity of infection of 1, and mitochondrial activity was measured by the MTT assay at the indicated time intervals.

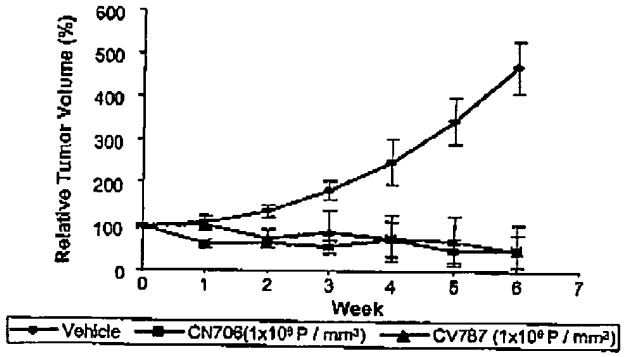

Fig. 6. Comparison of CN706 and CV787 i.t. injection activity toward LNCaP xenografts. *nu/nu* mice with s.c. LNCaP tumors (average size, 300 mm^3) were injected once into the tumor with 1×10^8 particles/mm^3 tumor of CN706 or 1×10^8 particles/mm^3 tumor of CV787.

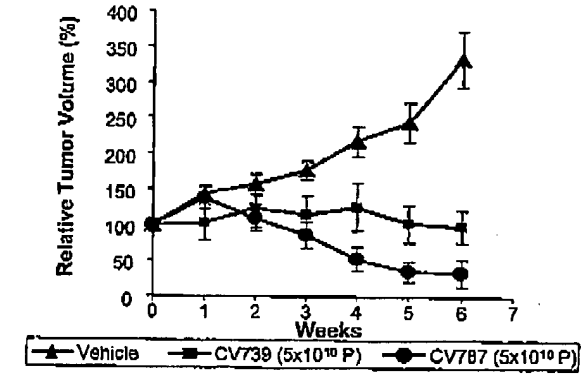

Fig. 7. Comparison of CV739 and CV787 i.v. injection activity toward LNCaP xenografts. *nu/nu* mice with s.c. LNCaP tumor xenografts (average size, 300 mm^3) were injected once into the tail vein with 5×10^{10} particles of CV739 or CV787.

the burst size of CN706 ranged from 3×10^3 to 1×10^4 in 293 cells and the PSA^+ cell line LNCaP; however, in all PSA^- cell lines, the burst size ranged from 1×10^1 to 8×10^1. The burst sizes of CV739 and CV787 were $\sim 10^4$ in 293 cells and the PSA^+ cell line LNCaP and were less than 1 to 1×10^{-2} in all PSA^- cell lines. Failure of CV787 to reach a burst size of 1 by 48 h following infection with a multiplicity of 2 indicates an essentially complete inability to replicate in cells lacking transcription factors that are capable of interacting with PSE. CV787 is capable of replicating but to an extremely limited extent in PSA^- cells, as shown by its growth curve in hMVEC cells (Fig. 3). In these cells, CV787 replicated 10–20-fold during 4 days following infection with a multiplicity of 2 pfu/cell, but in which the burst size, in agreement with the results presented above, failed to reach 1. In contrast, CV802 (wt Ad5) replicated 10^6-fold and reached a burst size of 10^4.

Specificity of CV787 was also shown by cell survival of PSA^- HBL-100 and OVCAR-3 cells, as measured by the MTT assay, compared with the destruction of PSA^+ LNCaP cells. Whereas CV802 destroyed all three cell types, CV787 only destroyed PSA^+ LNCaP cells (data not shown). Specific cell destruction was also measured in hMVEC monolayers infected for 10 days with multiplicities ranging from 0.01 to 10. Data similar to those previously published for CV764 (7) show that, even at an infecting multiplicity of 0.01, CV802 (wt Ad5) caused very substantial cytopathic effects; in contrast, CV787 caused minimal cytopathic effects in 10 days, even at an infecting multiplicity of 10 (data not shown). Together, these results confirm the conclusion that CV787 is almost totally attenuated for PSA^- cells but replicates normally in PSA^+ cells.

Increased Efficacy of CV787 Due to the Ad5 E3 region. The increased efficacy resulting from the incorporation of the Ad5 E3 region was first shown by *in vitro* tests. A representative plaque assay of CV739 ($E3^-$) and CV787 ($E3^+$) on 293 cells is shown in Fig. 4. Plaques of E3-deleted Ad5 are substantially smaller and less distinct than those of E3-containing adenovirus 10 days after infection. Plaques of CV787 appear more than 3-fold larger than plaques of CV739. $E3^-$ CN702 and $E3^-$ CN706 produced plaques similar to those shown for $E3^-$ CV739, whereas $E3^+$ CV802 produced plaques similar to those shown for $E3^+$ CV787 (data not shown). A similar picture of efficacy emerged when LNCaP cell survival was assessed by measuring mitochondrial activity (17). CV787 completely eliminated mitochondrial activity 7 days after infection, whereas CV739 cells still had 67% the mitochondrial activity of uninfected cells 7 days after infection (Fig. 5).

The increased efficacy of incorporation of the Ad5 E3 region was also shown *in vivo*, as measured in the LNCaP *nu/nu* mouse xenograft model. BALB/c *nu/nu* mice harboring s.c. 300-mm^3 LNCaP xenografts located on the back were injected either i.t. or i.v. into their tail veins with either vehicle (50 μl of PBS-10% glycerol) or the same volume of vehicle containing CN706, CV739, or CV787. Fig. 6 shows the result of a single i.t. treatment of LNCaP tumors with 1×10^8 particles/mm^3 tumor CN706 or 1×10^6 particles/mm^3 tumor CV787. Both viruses yielded the same degree of tumor reduction, implying a 100-fold increase in efficacy of CV787, compared with CN706. In addition, 1×10^8 particles/mm^3 tumor CV787 completely eliminated LNCaP tumors by a single i.t. injection (data not shown). Differential

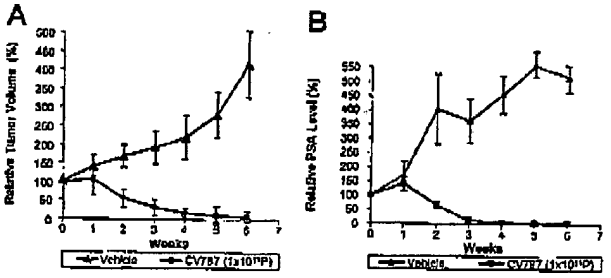

Fig. 8. LNCaP xenograft tumors in *nu/nu* mice following one i.v. tail vein injection of CV787. *A*, tumor size, measured weekly. *B*, serum PSA, measured weekly by immunoassay. *C*, replication of adenovirus in LNCaP tumors determined by immunohistochemistry with rabbit polyclonal antibody to Ad5.

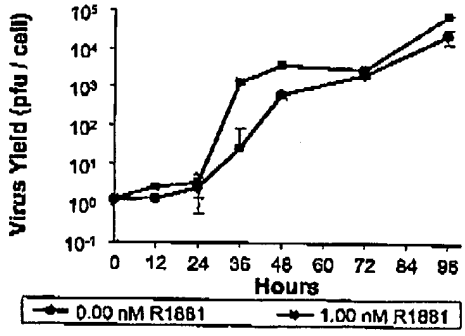

Fig. 9. Growth of CV787 in LNCaP cells with or without R1881. LNCaP cells were infected with CV787 at a multiplicity of infection of 2. Following adsorption, the cells were washed twice with PBS, and medium with or without R1881 was added. Duplicate cultures were harvested at the indicated time points and subjected to three cycles of freeze-thaw, and virus titers were determined in triplicate on 293 cells.

efficacy toward LNCaP tumors between CV739 and CV787 was also shown following a single i.v. administration of 5×10^{10} particles. Fig. 7 shows that CV739 could stop tumor growth at this dose level but that CV787 caused a 4-fold reduction in tumor volume.

i.v. Administration of CV787. Perhaps most importantly, CV787 could eliminate preexistent distantly located LNCaP tumors. Six weeks following a single i.v. injection of 1×10^{11} CV787 particles, the sizes of the tumors were reduced to less than 5% of their original size (Fig. 8*A*), and 8 of 14 mice were visually free of tumors. Those tumors that were still present were immunohistologically devoid of PSA (data not shown). The serum PSA levels in mice injected with buffer increased (Fig. 8*B*), whereas the levels in mice injected with CV787 decreased to ~5% of their starting values within 3 weeks. Virus replication within LNCaP xenografts could be shown at both 7 and 28 days after injection, as evidenced by Ad5 immunostaining (Fig. 8*C*). As controls, similar experiments were carried out with *nu/nu* mice carrying LoVo (colon cancer) or Hep3B (hepatoma) xenografts. These xenografts continued to grow normally following tail vein injection of CV787 (data not shown).

Finally, hormone-refractory patients continue hormone therapy, even if such hormone ablation therapy is no longer effective (2, 3). If CV787 is to be considered to treat end-stage metastatic hormone-refractory prostate cancer, it is important to know whether CV787 can grow in the absence of testosterone. Fig. 9 shows the one-step growth curve of CV787 in LNCaP cells in the presence of the stable but biologically active testosterone analogue R1881 at 1 nM and in the absence of R1881. CV787 grows normally in the absence of R1881 and achieved a burst size in excess of 10^4 pfu/cell.

In summary, CV787 is an ARCA that replicates like wt Ad5 in cells that express PSA but that is attenuated 10,000–100,000-fold with respect to replication in PSA^- cells. CV787 is highly cytopathogenic in PSA^+ cells and is capable of eliminating distantly located preexisting prostate tumors following i.v. injection. The addition of the Ad5 E3 region increases efficacy 10–100-fold both *in vitro* and *in vivo*. Furthermore, CV787 with the complete E3 region can be expected to resist many of the host antiviral MHC-1 defense mechanisms of wt Ad5 (15–17, 25). Finally, CV787 can replicate normally in the absence of testosterone and could, thereby, help patients continuing hormonal ablation therapy. CV787 is a potentially powerful therapeutic for human metastatic cancer.

Acknowledgments

We thank Young Kim, Heather Conners, and Andy Little for technical assistance. We also thank Dr. W.K. Joklik for suggestions in preparing and editing the manuscript.

References

1. Landis, S. H., Murray, T., Bolden, S., and Wingo, P. A. Cancer statistics, 1998. CA Cancer J. Clin., *48:* 6–29, 1998.
2. Small, E. J. Prostate cancer, incidence, management and outcomes. Drugs Aging, *13:* 71–81, 1998.
3. Bare, R. L., and Torti, F. M. Endocrine therapy of prostate cancer. Cancer Treat Res., *94:* 69–87, 1998.
4. Tyrrell, C. J., Kaisary, A. V., Iversen, P., Anderson, J. B., Baert, L., Tammela, T., Chamberlain, M., Webster, A., and Blackledge, G. A randomised comparison of "Casodex" (bicalutamide) 150 mg monotherapy *versus* castration in the treatment of metastatic and locally advanced prostate cancer. Eur. Urol., *33:* 447–456, 1998.
5. Schuur, E. R., Henderson, G. A., Kmetec, L. A., Miller, J. D., Lamparski, H. G., and Henderson, D. R. Prostate-specific antigen expression is regulated by an upstream enhancer. J. Biol. Chem., *271:* 7043–7051, 1996.
6. Rodriguez, R., Schuur, E. R., Lim, H. Y., Henderson, G. A., Simons, J. W., and Henderson, D. R. Prostate-attenuated replication competent adenovirus (ARCA) CN706: a selective cytotoxic for prostate-specific antigen positive prostate cancer cells. Cancer Res., *57:* 2559–2563, 1997.
7. Yu, D-C., Sukamoto, G. T., and Henderson, D. R. Identification of the transcriptional regulatory sequences of human kallikrein 2 and their use in the construction of calydon virus 764, an attenuated replication competent adenovirus for prostate cancer therapy. Cancer Res., *59:* 1498–1504, 1999.
8. Ben, A. J., Haddara, W., Prevec, L., and Graham, F. L. An efficient and flexible system for construction of adenovirus vectors with insertions or deletions in early regions 1 and 3. Proc. Natl. Acad. Sci. USA, *91:* 8802–8806, 1994.
9. Haj-Ahmad, Y., and Graham, F. L. Development of a helper-independent human adenovirus vector and its use in the transfer of the herpes simplex virus thymidine kinase gene. J. Virol., *57:* 267–274, 1986.
10. Ghosh-Choudhury, G., Haj-Ahmad, Y., Brinkley, P., Rudy, J., and Graham, F. L. Human adenovirus cloning vectors based on infectious bacterial plasmids. Gene, *50:* 161–171, 1986.
11. Graham, F. L. Adenoviruses as expression vectors and recombinant vaccines. Trends Biotechnol., *8:* 85–87, 1990.
12. Robbins, P. D., Tahara, H., and Ghivizzani, S. C. Viral vectors for gene therapy. Trends Biotechnol., *16:* 35–40, 1998.
13. Wivel, N. A., and Wilson, J. M. Methods of gene delivery. Hematol. Oncol. Clin. North Am., *12:* 483–501, 1998.
14. Ilan, Y., Droguett, G., Chowdhury, N. R., Li, Y., Sengupta, K., Thummala, N. R., Davidson, A., Chowdhury, J. R., and Horwitz, M. S. Insertion of the adenoviral E3 region into a recombinant viral vector prevents antiviral humoral and cellular immune responses and permits long-term gene expression. Proc. Natl. Acad. Sci. USA, *94:* 2587–2592, 1997.
15. Ginsberg, H. S., Lundholm-Beauchamp, U., Horswood, R. L., Pernis, B., Wold, W. S., Chanock, R. M., and Prince, G. A. Role of early region 3 (E3) in pathogenesis of adenovirus disease. Proc. Natl. Acad. Sci. USA, *86:* 3823–3827, 1989.
16. Wold, W. S., Tollefson, A. E., and Hermiston, T. W. E3 transcription unit of adenovirus. Curr. Top. Microbiol. Immunol., *199:* 237–274, 1995.
17. Tollefson, A. E., Ryerse, J. S., Scaria, A., Hermiston, T. W., and Wold, W. S. The E3–11.6-kDa adenovirus death protein (ADP) is required for efficient cell death: characterization of cells infected with adp mutants. Virology, *220:* 152–162, 1996.
18. Tollefson, A. E., Scaria, A., Hermiston, T. W., Ryerse, J. S., Wold, L. J., and Wold, W. S. The adenovirus death protein (E3–11.6K) is required at very late stages of infection for efficient cell lysis and release of adenovirus from infected cells. J. Virol., *70:* 2296–2306, 1996.
19. Hausmann, J., Ortmann, D., Witt, E., Veit, M., and Seidel, W. Adenovirus death protein, a transmembrane protein encoded in the E3 region, is palmitoylated at the cytoplasmic tail. Virology, *244:* 343–351, 1998.
20. Korner, H., and Burgert, H. G. Down-regulation of HLA antigens by the adenovirus type 2 E3/19K protein in a T-lymphoma cell line. J. Virol., *68:* 1442–1448, 1994.
21. Flomenberg, P., Gutierrez, E., and Hogan, K. T. Identification of class I MHC regions which bind to the adenovirus E3–19k protein. Mol. Immunol., *31:* 1277–1284, 1994.
22. Li, Y., Kang, J., and Horwitz, M. S. Interaction of an adenovirus E3 14.7-kilodalton protein with a novel tumor necrosis factor α-inducible cellular protein containing leucine zipper domains. Mol. Cell. Biol., *18:* 1601–1610, 1998.
23. Elsing, A., and Burgert, H. G. The adenovirus E3/10.4K-14.5K proteins down-modulate the apoptosis receptor Fas/Apo-1 by inducing its internalization. Proc. Natl. Acad. Sci. USA, *95:* 10072–10077, 1998.
24. Dimitrov, T., Krajcsi, P., Hermiston, T. W., Tollefson, A. E., Hannink, M., and Wold, W. S. Adenovirus E3–10.4K/14.5K protein complex inhibits tumor necrosis factor-induced translocation of cytosolic phospholipase A2 to membranes. J. Virol., *71:* 2830–2837, 1997.
25. Vinogradova, O., Carlin, C., Sonnichsen, F. D., and Sanders, C. R., II. A membrane setting for the sorting motifs present in the adenovirus E3–13.7 protein which down-regulates the epidermal growth factor receptor. J. Biol. Chem., *273:* 17343–17350, 1998.
26. Greenberg, N. M., DeMayo, F. J., Sheppard, P. C., Barrios, R., Lebovitz, R., Finegold, M., Angelopoulou, R., Dodd, J. G., Duckworth, M. L., Rosen, J. M., and Matusik, R. J. The rat probasin gene promoter directs hormonally and developmentally regulated expression of a heterologous gene specifically to the prostate in transgenic mice. Mol. Endocrinol., *8:* 230–239, 1994.
27. Yan, Y., Sheppard, P. C., Kasper, S., Lin, L., Hoare, S., Kapoor, A., Dodd, J. G., Duckworth, M. L., and Matusik, R. J. Large fragment of the probasin promoter targets high levels of transgene expression to the prostate of transgenic mice. Prostate, *32:* 129–139, 1997.
28. Brookes, D. E., Zandvliet, D., Watt, F., Russell, P. J., and Molloy, P. L. Relative activity and specificity of promoters from prostate-expressed genes. Prostate, *35:* 18–26, 1998.
29. McKinnon, R. D., Bacchetti, S., and Graham, F. L. Tn5 mutagenesis of the transforming genes of human adenovirus type 5. Gene, *19:* 33–42, 1982.
30. Graham, F. L., Smiley, J., Russell, W. C., and Nairn, R. Characteristics of a human cell line transformed by DNA from human adenovirus type 5. J. Gen. Virol., *36:* 59–74, 1977.

0022-3565/96/2792-1026$03.00/0
THE JOURNAL OF PHARMACOLOGY AND EXPERIMENTAL THERAPEUTICS
Copyright © 1996 by The American Society for Pharmacology and Experimental Therapeutics
JPET 279:1026-1034, 1996

Vol. 279, No. 2
Printed in U.S.A.

JPET PHARMACOLOGY AND EXPERIMENTAL THERAPEUTICS aspet

Targeting of Antibody-Conjugated Plasminogen Activators to the Pulmonary Vasculature

VLADIMIR R. MUZYKANTOV, ELLIOT S. BARNATHAN, ELENA N. ATOCHINA, ALICE KUO, SERGEI M. DANILOV and ARON B. FISHER

Institute for Environmental Medicine and Department of Medicine, University of Pennsylvania (V.R.M., E.S.B., E.N.A., A.K., A.B.F.) and Institute of Experimental Cardiology, Russian Cardiology Research Center, Moscow, Russia (S.M.D.)

Accepted for publication July 25, 1996

ABSTRACT

Thrombolytic therapy has not been widely used for pulmonary embolism due to less than optimal results with conventional plasminogen activators. We propose a new approach to deliver plasminogen activators to the luminal surface of the pulmonary vasculature to potentially improve dissolution of pulmonary thromboemboli. Our previous studies have documented that a monoclonal antibody (mAb) to angiotensin-converting enzyme (anti-angiotensin-converting enzyme mAb 9B9) accumulates in the lungs of various animal species after systemic administration. We coupled ^{125}I-labeled biotinylated plasminogen activators (single-chain urokinase plasminogen activator, tissue-type plasminogen activator and streptokinase) to biotinylated mAb 9B9, using streptavidin as a cross-linker. The fibrinolytic activity of plasminogen activators was not changed significantly by either biotinylation or by coupling to streptavidin. Antibody-conjugated plasminogen activators bind to the antigen immobilized in plastic wells and provide lysis of fibrin clots formed in these wells. Therefore, antibody-conjugated plasminogen activators bound to their target antigen retain their capacity to activate plasminogen. One hour after i.v. injection of mAb 9B9-conjugated radiolabeled biotinylated single-chain urokinase plasminogen activator, biotinylated tissue-type plasminogen activator or biotinylated-streptokinase in rats, the level of radiolabel was 7.4 ± 0.8, 5.9 ± 0.4 and 3.6 ± 0.4% of injected dose/g (ID/g) of lung tissue *vs.* 0.5 ± 0.01, 0.3 ± 0.01 and 0.6 ± 0.3% ID/g after injection of the same activators conjugated with control mouse IgG ($P < .01$ in all cases). Injection of mAb 9B9-conjugated radiolabeled plasminogen activator led to its rapid pulmonary uptake with a peak value 6.2 ± 1.2% ID/g attained 3 hr after injection. One day later, 2.2 ± 0.5% of the injected radioactivity was found per gram of lung tissue, although the blood level was 0.13 ± 0.03% ID/g (lung/blood ratio 16.7 ± 0.3). Therefore, conjugation of plasminogen activators with anti-angiotensin-converting enzyme mAb 9B9 provides their specific targeting to and prolonged association with the pulmonary vasculature. These results provide a basis for study of the local pulmonary fibrinolysis by mAb 9B9-conjugated plasminogen activators.

The pulmonary vasculature is a frequent target for occlusion by thromboemboli associated with various diseases and syndromes. Plasminogen activators are currently used for dissolution of intrapulmonary thromboemboli (Prewitt, 1991). These fibrinolytics, however, possess no specific affinity for the pulmonary vasculature and undergo rapid inactivation and elimination from the bloodstream (Verstraete and Lijnen, 1994). This may lead to less effective therapy. Compensation for this using high doses is associated with occasional but often serious bleeding complications. Current methods for the delivery of plasminogen activators (targeting to fibrin clots and local intrapulmonary infusion via catheter) do not provide prolonged association of plasminogen activators with the luminal surface of the pulmonary vasculature.

Received for publication May 9, 1996.

Specific, effective and safe therapy for pulmonary thromboembolism may be facilitated by a mechanism that 1) delivers fibrinolytic agent preferentially to the lung after systemic injection and 2) causes it to be present at the luminal surface of the pulmonary vasculature in an active form for a prolonged period of time. This might enhance fibrinolytic potential of the pulmonary vasculature and could, therefore, be useful for the prevention and/or treatment of a wide spectrum of cardiovascular and pulmonary diseases and syndromes associated with or manifested by pulmonary thromboembolism.

To develop such a strategy, plasminogen activators could be chemically coupled to a carrier possessing preferential affinity to the luminal surface of the pulmonary vasculature. We use a monoclonal antibody to ACE as such an affinity carrier. ACE is a carboxidipeptidase localized on the luminal

ABBREVIATIONS: ACE, angiotensin-converting enzyme; mAb, monoclonal antibody; PA, plasminogen activator; scuPA, single chain urokinase plasminogen activator; tPA, tissue-type plasminogen activator; BSA, bovine serum albumin; PBS, phosphate buffered saline; PBS-BSA, PBS containing 2 mg/ml BSA; %ID/g, percent of injected dose per gram of tissue; b-tPA, b-scuPA, b-streptokinase, b-IgG and b-mAb 9B9, biotinylated derivatives of these proteins; BxNHS, 6-biotinylamidocaproic acid N-hydroxysuccinimide ester.

surface of endothelial cells (Erdos, 1990). Lung contains a large portion of the total amount of ACE in the body and, importantly, endothelial ACE is accessible from the bloodstream (Caldwell *et al.*, 1976). Our previous studies documented that radiolabeled anti-ACE mAb 9B9 accumulates in the lungs of various animal species, including humans, after i.v., intraarterially and i.p. injections (Danilov *et al.*, 1991; Muzykantov and Danilov, 1995). Administration of mAb 9B9 appears to be safe, because this antibody does not fix complement, does not inhibit ACE and does not damage endothelium in culture or *in vivo* (Danilov *et al.*, 1991, 1994; Muzykantov and Danilov, 1995). Biotinylated mAb 9B9 provides pulmonary targeting of streptavidin and biotinylated enzymes conjugated with b-mAb 9B9 via streptavidin (Muzykantov *et al.*, 1994, 1995, 1996a).

Based on these characteristics of mAb 9B9, we hypothesized that conjugation of plasminogen activators with mAb 9B9 will provide their preferential pulmonary targeting. To test our hypothesis, we explored three different plasminogen activators: single chain urokinase plasminogen activator, tissue-type plasminogen activator and streptokinase. These plasminogen activators differ in their rate of blood clearance, inactivation and mechanisms of plasminogen activation (Verstraete and Lijnen, 1994; Plow *et al.*, 1995). None of them accumulate in the lungs after i.v. injection in animals. We describe biotinylation of plasminogen activators, their conjugation with biotinylated mAb 9B9 via streptavidin crosslinking and functional properties of antibody-conjugated plasminogen activators *in vitro*. We also describe the biodistribution and pulmonary targeting of antibody-conjugated plasminogen activators after systemic administration in laboratory animals.

Materials and methods

scuPA was obtained as a gift from J. Henkin (Abbott Laboratories, Abbott Park, IL). tPA was a gift from Genentech (San Francisco, CA), human plasminogen was from Chromogenix AB (Molndel, Sweden). Streptokinase, normal rabbit IgG, human fibrinogen, thrombin, BSA, DMF and chemicals for buffer solutions were from Sigma Chemical Co. (St. Louis, MO). Normal mouse IgG, streptavidin and BxNHS were from Calbiochem (San Diego, CA). Chromogenic substrate S2251 was from Kabi Vitrum. Iodogen and rabbit polyclonal antibody directed against mouse immunoglobulin were from Pierce Chemical Co. (Rockford, IL), ^{125}Iodine was from Amersham Corp. (Arlington Heights, IL). Male Sprague-Dawley rats (200–250 g) were from Charles River, N.Y. Mouse mAb to human angiotensin-converting enzyme, anti-ACE mAb 9B9 (IgG_1 isotype) was produced and characterized earlier (Danilov *et al.*, 1991, Muzykantov and Danilov, 1995).

Biotinylation of proteins. For biotinylation of plasminogen activators and antibody we used BxNHS, providing a 6-Angstrom spacer between the modified amino group of the protein and biotin residue covalently coupled to the protein molecule (Wilchek and Bayer, 1988). The additional steric freedom provided by the spacer allows more effective interactions of biotin-binding sites of streptavidin with biotin residues coupled to biotinylated proteins. The biotinylation procedure was performed by incubation of the protein (0.1–1 mg/ml in PBS, 7.4) with fresh solution of BxNHS in DMF, as described earlier (Muzykantov *et al.*, 1995). Previously we have demonstrated that biotinylation at a 10-fold molar excess of BxNHS provides coupling of streptavidin-accessible biotin residues to streptokinase (Muzykantov *et al.*, 1986), immunoglobulins (Muzykantov *et al.*, 1995), catalase and SOD (Muzykantov *et al.*, 1996a) without a marked reduction of their functional activities. To estimate the optimal procedure for tPA biotinylation, tPA was incubated with BxNHS at biotin/tPA molar ratios of 0 to 20 for 1 hr at 4°C. Streptokinase, scuPA, mAb 9B9, and immunoglobulins were biotinylated by the same protocol at a biotin/protein molar ratio of 10. Excess biotin ester was eliminated by dialysis against PBS, pH 7.4. Biotinylated plasminogen activators, as well as nonmodified human fibrinogen and streptavidin were radioiodinated using the Iodogen procedure according to manufacturer's recommendations.

To assess the streptavidin-binding capacity of biotinylated tPA, b-tPA was immobilized in the plastic wells of a 96-well microtest plate by overnight incubation at 4°C (0.1 mg/ml of b-tPA in PBS, pH 7.4, 100 μl/well). After elimination of nonbound b-tPA, wells were incubated with BSA to block nonspecific binding sites. Indicated amounts of radiolabeled streptavidin in PBS-BSA were incubated in b-tPA-coated wells, as well as in albumin- and nonbiotinylated tPA-coated wells for 1 hr at room temperature. After elimination of nonbound radiolabeled streptavidin, radioactivity in wells was determined in a gamma-counter. To confirm the specificity of the interaction between streptavidin and b-tPA, radiolabeled streptavidin was preincubated with nonbiotinylated tPA or with biotin and then its binding in the wells coated with b-tPA or with tPA was studied as described.

To assess the binding of radiolabeled b-PA to streptavidin, we immobilized streptavidin in the wells of a microtest plate by overnight incubation at 4°C (0.1 mg/ml streptavidin in PBS, pH 7.4, 100 μl/well). After elimination of nonbound streptavidin, wells were incubated with BSA to block nonspecific binding sites. Indicated amounts of radiolabeled b-PA in PBS-BSA were incubated in streptavidin-coated wells, as well as in albumin-coated wells (negative control for specific binding) for 1 hr at room temperature. After elimination of nonbound b-PA, radioactivity in wells was determined in a gamma-counter.

Assessment of fibrinolytic activity. Preformed fibrin clot containing plasminogen was prepared prior to addition of plasminogen activators. A freshly prepared solution of human fibrinogen (2 mg/ml in Krebs-Ringer buffer, pH 7.4) was filtered and mixed with human plasminogen (final concentration 50 nM) and thrombin (final concentration 1 μg/ml). The mixture was rapidly poured on the flat plastic surface (Petri dish or covering lid of multi-well) and incubated for 20 min at room temperature to form a fibrin gel of 3-mm thickness. The indicated amounts of plasminogen activators were applied to the surface of the fibrin gel; the gel was then incubated at 37°C for 90 min. After washing with water, the gel was incubated at 4°C with trypan blue solution to counterstain zones of fibrinolysis. The area of each zone of lysis was determined. In some experiments, normal human plasma was used as a source of plasminogen instead of pure plasminogen. Assessment of chromogenic substrate cleavage was performed in accordance with previously described protocol, using S-2251 substrate (Barnathan *et al.*, 1988).

Targeting of biotinylated plasminogen activator to immobilized streptavidin and fibrinolysis by streptavidin-bound plasminogen activator. This study was performed according to an experimental design described previously (Muzykantov *et al.*, 1986). Briefly, two drops of streptavidin solution (10 and 30 μl, 0.1 mg/ml each) were placed on the bottom of a plastic Petri dish. Overnight incubation at 4°C provides local immobilization of streptavidin in areas covered by streptavidin solution. After elimination of nonbound streptavidin, the rest of the bottom was coated with albumin, by addition of 3 ml PBS-BSA per dish. b-PA was incubated in dishes in 3 ml of PBS-BSA for 1 hr at room temperature. Therefore, during this incubation b-PA has contact with both target (streptavidin-coated) and nontarget (albumin-coated) surfaces. After elimination of nonbound b-PA, a freshly prepared mixture of fibrinogen, plasminogen and thrombin was poured in the Petri dish (the final concentrations of ingredients are indicated in a previous paragraph). After a 20-min incubation at room temperature, dishes with a formed fibrin gel were further incubated for 90 min at 37°C, washed with water and counterstained with trypan blue.

Preparation of b-PA/streptavidin/b-antibody complex. To construct the tri-molecular heteropolymer complex b-PA/streptavidin/b-antibody we used a two-step procedure described in our previous work (Muzykantov *et al.*, 1996a). First, radiolabeled b-PA was incubated with streptavidin for 1 hr at 4°C at molar ratios of streptavidin to b-PA in the range between 0 and 16. This procedure provides tight association of b-PA with streptavidin. Because streptavidin possesses four biotin-binding sites, bi-molecular complexes formed at an appropriate molar ratio may possess residual biotin-binding sites on streptavidin and, therefore, bind other biotinylated proteins (biotinylated antibodies). To estimate the optimal molar ratio streptavidin/b-PA that yields a bi-molecular complex with high biotin-binding capacity, we studied binding of ^{125}I-labeled b-PA/streptavidin complexes to immobilized b-IgG. b-IgG was immobilized in microtest plates by overnight incubation of b-IgG solution (0.1 mg/ml in PBS, 7.4). After elimination of nonbound b-IgG and incubation with albumin to block nonspecific binding, wells were incubated with ^{125}I-labeled b-PA/streptavidin complexes formed at various molar ratios streptavidin/b-PA. After a 1-hr incubation and washing of nonbound complexes, the radioactivity in wells was determined. The optimal ratio was determined to be two molecules of streptavidin per one molecule of biotinylated plasminogen activator (see "Results"). Accordingly, we conjugated b-PA with streptavidin at this molar ratio in all subsequent experiments. In a second step, bi-molecular complexes ^{125}I-labeled b-PA/streptavidin were incubated for 1 hr at 4°C with biotinylated immunoglobulins to form tri-molecular complexes ^{125}I-labeled b-PA/streptavidin/b-antibody, as described previously (Muzykantov *et al.*, 1996a). Gel-filtration on Sephacryl S-200 was used to characterize tri-molecular complexes, as described previously (Muzykantov *et al.*, 1994, 1996a).

Immunotargeting of antibody-PA complex to immobilized antigen in vitro and lysis of fibrin clot by antibody-PA complex bound to immobilized antigen. In this part of the study we used a model antigen and antibody pair. Accordingly, normal mouse IgG (immobilized in plastic wells of multiwell plates as described above) was used as the antigen and biotinylated rabbit polyclonal antibody to mouse IgG was used as the antibody. Biotinylated plasminogen activators were conjugated with biotinylated rabbit antibody as described above. In a series of control experiments, the same b-PA were conjugated with biotinylated nonspecific rabbit IgG and these conjugates were used as a nonimmune counterparts. Tri-molecular complexes b-PA/streptavidin/b-antibody were added in the antigen-coated wells or in BSA-coated wells (300 ng/well). The same amount of nonimmune counterparts (300 ng/well), *i.e.*, plasminogen activators conjugated with control rabbit IgG, were added in a parallel antigen- or BSA-coated wells. After a 1-hr incubation at room temperature, nonbound complexes were washed out. One ml of a fresh solution of radioiodinated fibrinogen mixed with plasminogen and thrombin was poured into each well. After a 20-min incubation at room temperature to form a fibrin gel, plates were incubated at 37°C for 90 min. Then 1 ml of saline was added to each well and radioactivity in 0.5 ml supernatant was determined in a gamma-counter.

In vivo administration of radiolabeled plasminogen activators conjugated with antibody or IgG. The general experimental design for this part of the study has been described in our previous publications (Danilov *et al.*, 1991, 1994; Muzykantov and Danilov, 1995). Normal anesthetized Sprague-Dawley rats received injections i.v. with 1 μg of radiolabeled probes. Radiolabeled biotinylated plasminogen activators conjugated with b-mAb 9B9 or with b-IgG via streptavidin, as well as nonconjugated b-PA and nonmodified radiolabeled PA, were used as probes. At indicated time after injection, animals were killed to obtain samples of blood and internal organs. Radioactivity in tissues was determined in a gamma-counter. The biodistribution of each probe was characterized by the % ID/g and the ratio of radioactivity per gram of tissue to that of blood (tissue/blood ratio).

Results

In this study we explored the use of streptavidin-biotin cross-linker as a general method for conjugation of various plasminogen activators with mAb 9B9. We used BxNHS (long arm derivative) to obtain covalent coupling of biotin residues to amino groups of plasminogen activators and mAb 9B9. Figure 1A shows that: 1) streptavidin does not bind to

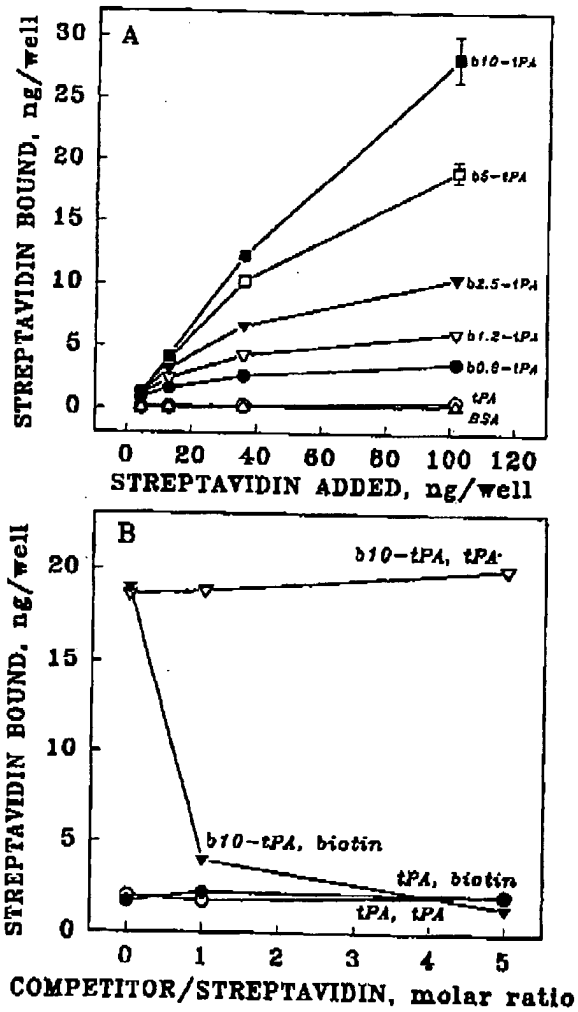

Fig. 1. Binding of radiolabeled streptavidin to biotinylated tPA. A, Tissue-type plasminogen activator has been modified by BxNHS at molar ratios BxNHS/tPA 0.5 (closed circles), 1.2 (open triangles), 2.5 (closed triangles), 5 (open squares) or 10 (closed squares). Biotinylated tPA, as well as nonmodified tPA (open circles) was immobilized in plastic wells and binding of radiolabeled streptavidin in the wells has been assessed as described in "Materials and Methods." BSA-coated wells were used as a negative control (open triangles). B, Radiolabeled streptavidin has been preincubated for 1 hr at room temperature with indicated molar excess of biotin (closed triangles and circles) or nonmodified tPA (open triangles and circles). Then binding of radiolabeled streptavidin was assessed in the wells coated with biotinylated tPA (b10-tPA, triangles) or with nonmodified tPA (circles). Binding of streptavidin to b-tPA was completely inhibited by biotin, while tPA has no effect. In each experiment the binding has been performed in triplicate wells. The data are shown as mean ± S.D., $n = 3$.

wells coated with nonbiotinylated tPA, as well as to BSA-coated wells; 2) it binds to the wells coated with biotinylated tPA and 3) tPA biotinylated at higher biotin/tPA molar ratio provides more binding sites for streptavidin. Streptavidin binding to immobilized b-tPA was not affected by preincubation of radiolabeled streptavidin with nonbiotinylated tPA, whereas biotin completely blocked streptavidin binding (fig. 1B). These data confirm the specificity of interaction between streptavidin and b-tPA and directly document that this interaction is mediated by biotin residues coupled to tPA. Vice versa, radiolabeled b-tPA binds to streptavidin-coated wells by specific and saturable fashion (fig. 2). Radiolabeled biotinylated scuPA and streptokinase demonstrated similar streptavidin-binding properties (not shown).

As we have documented previously, biotinylation of streptokinase at biotin/streptokinase molar ratio higher than 10 leads to a detectable reduction of its fibrinolytic activity (Muzykantov *et al.*, 1986). In support of this previous observation, our present data demonstrated that biotinylation of tPA at a biotin/tPA molar ratio of 20 led to a 30% reduction of its activity assessed by cleavage of a chromogenic substrate. However, tPA biotinylation at 10-fold molar excess of BxNHS does not alter the activity of tPA and, moreover, conjugation of b-tPA with streptavidin does not lead to a detectable reduction of b-tPA activity (not shown). To estimate further the fibrinolytic activity of biotinylated plasminogen activators, we have examined lysis of preformed fibrin clots, containing plasminogen (fig. 3). The same rate of lysis of fibrin gel was induced by streptokinase, streptokinase biotinylated at 10-fold molar excess of BxNHS (b-streptokinase) and b-streptokinase conjugated with streptavidin. Similar results were obtained with b-tPA and b-scuPA (not shown). Fibrinolysis also occurred when normal human plasma was used as a source of plasminogen instead of human purified plasminogen (not shown). These results document that neither biotinylation nor conjugation with streptavidin significantly reduce the capacity of plasminogen activators to activate plasminogen or to induce fibrinolysis.

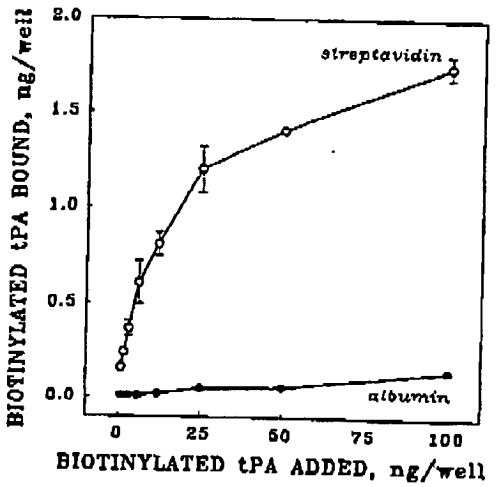

Fig. 2. Binding of radiolabeled b-tPA to immobilized streptavidin. ^{125}I-labeled b-tPA was incubated in plastic wells coated with streptavidin (open circles) or in albumin-coated wells (closed circles). After a 1-hr incubation and elimination of unbound b-tPA, amount of bound radioiodinated b-tPA in wells was determined. Nonbiotinylated radiolabeled t-PA did not bind to either streptavidin-coated wells or albumin-coated wells (not shown). In each experiment the binding has been performed in triplicates, the data are shown as mean ± S.D., $n = 3$.

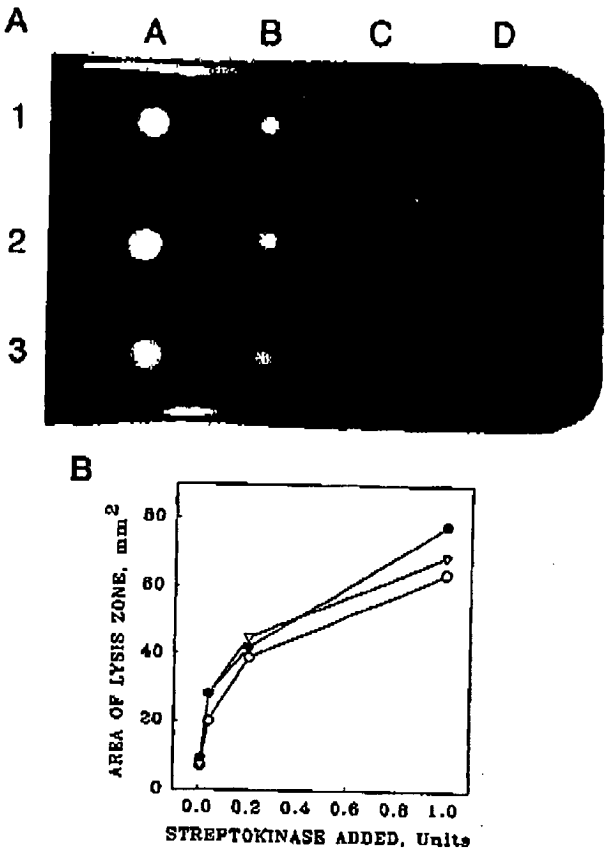

Fig. 3. Biotinylation and conjugation with streptavidin do not affect fibrinolytic activity of plasminogen activator. Fibrin gel was formed by mixing human fibrinogen (2 mg/ml), plasminogen (50 nM) and thrombin (1 μg/ml). Equal amounts of each streptokinase preparation were placed on the surface of fibrin gel. After a 90-min incubation at 37°C, diameters of lytic zones were measured and surface area of fibrinolysis was calculated. A shows the fibrin gel counterstained with trypan blue after incubation with streptokinase (lane 1), b-streptokinase (lane 2) and b-streptokinase conjugated with streptavidin (lane 3). Amount of streptokinase applied on the surface of the gel was 1000 mU (A), 200 mU (B), 40 mU (C) and 8 mU (D). B shows calculated results of experiment shown in panel A. The symbols are nonmodified streptokinase (open circles), b-streptokinase (closed circles) and b-streptokinase conjugated with streptavidin (triangles).

In the next series of experiments, we asked whether plasminogen activator bound to the target surface retains its ability to induce fibrinolysis. To address this issue, we immobilized streptavidin on two zones of the bottom of plastic Petri dishes. The rest of the bottom was coated with BSA and thus represented a nontarget surface. Biotinylated streptokinase was incubated in the dish (100 U/dish), thus contacting with both target and nontarget surfaces. After elimination of nonbound b-streptokinase, plasminogen-containing fibrin gel was formed in the dishes. Figure 4 demonstrates that incubation of such a dish at 37°C leads to lysis of fibrin gel exactly in the areas covering target zones. Areas of fibrinolysis were 28 and 57 mm^2 over small and large streptavidin targets,

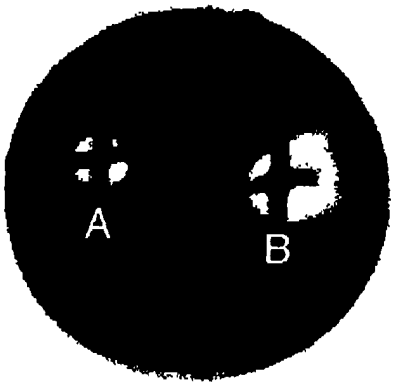

Fig. 4. Local fibrinolysis induced by b-streptokinase targeted to immobilized streptavidin. Streptavidin was immobilized in two areas of the bottom of plastic Petri dish marked with crosses, by overnight incubation of 10 μl (A) and 30 μl (B) of a streptavidin-containing solution. The rest of the bottom was coated with albumin. Biotinylated streptokinase (100 U) was incubated in the dish for 1 hr at room temperature. After elimination of nonbound b-streptokinase, fibrin gel was formed in the dish as described in the legend to figure 2. After a 90-min incubation at 37°C, the gel was washed with water and counterstained with trypan blue. Note that fibrin gel was lysed only over the target areas and that size of the lytic zone corresponds to size of the targets (28 mm^2 over zone A and 57 mm^2 over zone B).

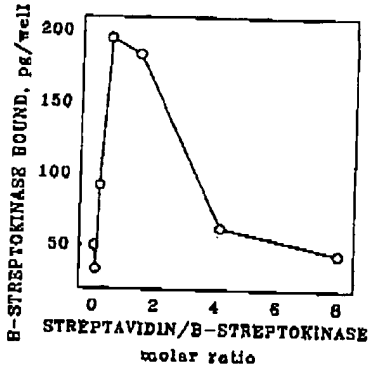

Fig. 5. Assessment of biotin-binding capacity of bi-molecular complex b-streptokinase/streptavidin. Radiolabeled b-streptokinase was incubated for 1 hr with streptavidin at indicated molar ratios. Then b-streptokinase/streptavidin complexes were incubated for 1 hr at room temperature in plastic wells coated with biotinylated IgG. After elimination of nonbound complexes, amount of bound b-streptokinase in wells was determined by counting of radioactivity. Binding of b-streptokinase/streptavidin complexes in albumin-coated wells was lower than 20 pg/well for all b-streptokinase/streptavidin complexes (not shown).

respectively. Similar result has been obtained with b-scuPA and b-tPA (not shown). Thus, biotinylated plasminogen activators 1) bind specifically to immobilized streptavidin and, 2) induce effective fibrinolysis in the target zone, despite steric limitations imposed by their attachment to the target.

To conjugate biotinylated plasminogen activators with biotinylated antibody, we used a two-step procedure, which we have developed for conjugation of biotinylated antioxidant enzymes with biotinylated antibody (Muzykantov *et al.*, 1996a). First, incubation of b-PA with streptavidin creates the bi-molecular complex b-PA/streptavidin. At this step we have to estimate the optimal molar ratio between b-PA and streptavidin. Bi-molecular complex b-protein/streptavidin, formed at such an optimal molar ratio, possesses high residual biotin-binding capacity that permits consequent conjugation with biotinylated antibody. To estimate this optimal ratio, we examined the interaction of ^{125}I-labeled b-PA/streptavidin complexes, formed at various molar ratios, with immobilized biotinylated IgG. Figure 5 shows that bimolecular complex b-streptokinase/streptavidin formed at a streptavidin/b-streptokinase molar ratio of 2 possesses a maximal binding capacity toward b-IgG. Neither b-streptokinase nor b-streptokinase/streptavidin complex formed at very low input of streptavidin bind to immobilized b-IgG. This confirms the specificity of cross-linking of two different biotinylated proteins (b-streptokinase and b-IgG) via streptavidin. Similar results were obtained with other biotinylated plasminogen activators (not shown). Therefore, 2-fold molar excess of streptavidin during its conjugation with b-PA provides bi-molecular complexes that can be further conjugated with biotinylated antibody. At lower streptavidin input most of its biotin-binding sites are preoccupied with biotin residues coupled with plasminogen activators and such complexes do not bind biotinylated IgG. Conjugation at higher excess of streptavidin would require an additional procedure to separate nonreacted streptavidin. In the second step, a 2-fold excess of biotinylated antibody (or b-IgG for control experiments) was incubated with bi-molecular complex b-PA/streptavidin. This procedure generates a tri-molecular complex b-PA/streptavidin/b-antibody. After gel-filtration of tri-molecular complexes on Sephacryl S-200, 80% of radiolabeled b-PA was eluted in a single peak corresponding to the exclusion volume of the column (not shown). Thus, the conjugation procedure yields a tri-molecular complex with a high molecular weight (>500 kD).

To examine the fibrinolytic potential of antibody-conjugated plasminogen activators, we conjugated b-scuPA and b-streptokinase with biotinylated rabbit polyclonal antibody to mouse IgG. Mouse IgG (used as a model antigen in this part of study), had been immobilized in the wells of a multi-well plate. Plasminogen activators were conjugated with biotinylated antibody to mouse IgG or with biotinylated control rabbit IgG. Antibody-conjugated or IgG-conjugated PA were incubated in the antigen-coated wells or in the albumin-coated wells. After elimination of nonbound conjugates, a solution of radiolabeled fibrinogen containing plasminogen and thrombin was added into each well, to form radiolabeled clots in the wells. Figure 6 shows that fibrinolysis (measured by release of radiolabel in the supernatants) occurred in the wells coated with antigen and incubated with antibody-conjugated b-scuPA or b-streptokinase (Ab/Ag wells). Nonimmune counterparts, as well as antibody-conjugated plasminogen activators incubated in albumin-coated wells, did not induce fibrinolysis. Therefore, immunotargeting of plasminogen activators to antigen-coated surfaces leads to plasminogen conversion and fibrinolysis in the target area.

To study the biodistribution of antibody-conjugated plasminogen activators, we injected rats i.v. with tri-molecular complexes ^{125}I-labeled b-PA/streptavidin/b-mAb 9B9. Complexes containing nonspecific mouse IgG were used to control the specificity of the targeting. Figure 7 shows that all plasminogen activators conjugated with mAb 9B9 accumulate in the rat lungs, whereas IgG-conjugated plasminogen activa-

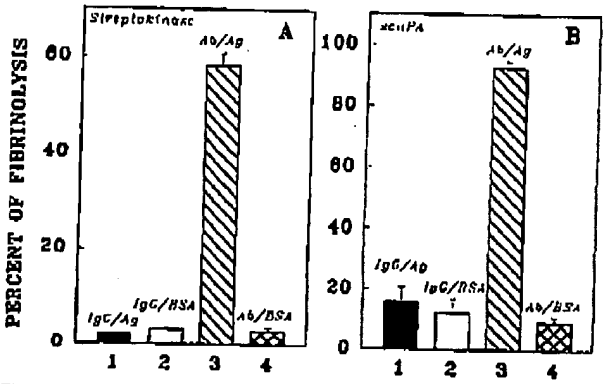

Fig. 6. Targeting of antibody-conjugated plasminogen activators to immobilized antigen leads to fibrinolysis in the antigen-coated wells. Tri-molecular complexes b-streptokinase/streptavidin/b-antibody (A) and b-scuPA/streptavidin/b-antibody (B) were prepared as described in "Materials and Methods." Biotinylated rabbit polyclonal antibody directed against mouse IgG was used as a model antibody in this experiment. To control the specificity of targeting and fibrinolysis, biotinylated plasminogen activators were conjugated with biotinylated normal rabbit IgG using the same method. Antibody-conjugated plasminogen activators (Ab, bars 3 and 4) or nonimmune counterparts (IgG, bars 1 and 2) were incubated in the antigen-coated wells (Ag, bars 1 and 3) or in wells coated with albumin (BSA, bars 2 and 4). After elimination of nonbound complexes, fibrin clots containing plasminogen and radiolabeled fibrin were formed in all wells as described in "Materials and Methods." After a 90-min incubation at 37°C, the fibrinolysis was determined by counting of radioactivity in supernatants. The data are presented as percent of release of radiolabel from gels to supernatants in three independent wells for each preparation. (mean ± S.D., $n = 3$).

tors do not accumulate in the lungs. One hour after i.v. injection of mAb 9B9-conjugated b-scuPA, b-tPA and b-streptokinase, the percent of injected radioactivity found in the lung was 7.4 ± 0.8, 5.9 ± 0.4 and 3.6 ± 0.4% of the injected dose/gram of lung tissue *vs.* 0.5 ± 0.01, 0.3 ± 0.01 and 0.6 ± 0.3% after injection of the same activators conjugated with control mouse IgG ($n = 3$ and $P < .01$ in all cases). The lung/blood ratio of tissue radioactivity was equal to 4.7 ± 0.4, 10.8 ± 1.3 and 7.8 ± 0.8 one hr after injection of mAb 9B9-conjugated b-scuPA, b-tPA and b-streptokinase. In contrast, the lung/blood ratio of radioactivity after injection of nonimmune counterparts was consistently <0.5. Therefore, conjugation with anti-ACE mAb 9B9 provides 10 to 20 times higher pulmonary uptake of plasminogen activators, as compared with nonimmune counterparts.

Figure 8 demonstrates the kinetics of the pulmonary uptake of tri-molecular complex ^{125}I-labeled b-tPA/streptavidin/b-mAb 9B9, as well as nonconjugated ^{125}I-labeled tPA in rats after i.v. injection. Nonconjugated tPA did not accumulate in the lung (0.23 ± 0.09% of the injected dose/g 1 hr after injection). In contrast, as soon as 5 min after i.v. injection of antibody-conjugated tPA, 4.3 ± 0.8% of injected radioactivity was detected in the lung tissue (4.8 ± 0.9% ID/g, lung/blood ratio 3.1 ± 0.9). Maximal pulmonary accumulation (6.2 ± 1.1% ID/g) was observed 3 hr after injection; the lung/blood ratio also was maximal at this time (19.3 ± 4.1). One day after injection, 2.1 ± 0.5% of ID/g was still detected in the lung tissue and the lung/blood ratio was equal to 16.7 ± 0.34. Thus, mAb 9B9-conjugated tPA displays rapid and prolonged pulmonary uptake.

Figure 9 shows the biodistribution of tri-molecular complex ^{125}I-labeled b-scuPA/streptavidin/b-mAb 9B9, as well as nonimmune counterpart, in tissues 1 hr after i.v. injection in rats. This result confirms the selectivity of the targeting of mAb 9B9-conjugated plasminogen activator to the pulmonary vasculature. The tissue/blood ratio was significantly higher than 1 only in the lung tissue (4.7 ± 0.4 one hr after injection), although in all other tissues this parameter was consistently <1. There was no pulmonary uptake of IgG-conjugated plasminogen activator (0.5 ± 0.01% ID/g).

Discussion

There are several plasminogen activators currently suggested for treatment of thromboembolism (Prewitt, 1991). Streptokinase binds plasminogen and induces its autoactivation and conversion into plasmin by autolysis (Serrano *et al.*, 1996). tPA and uPA are proteases specific for plasminogen (Verstraete and Lijnen, 1994; Plow *et al.*, 1995). Single chain urokinase (scuPA) is a zymogen that can be activated by plasmin (Plow *et al.*, 1995), and, at lesser rate, by the cellular receptor for urokinase (Higazi *et al.*, 1995). Plasmin formed by proteolytic activation of plasminogen is a protease with broad specificity, degrading fibrin and components of extracellular matrix (Plow *et al.*, 1995). However, plasminogen activators and their derivatives do not possess a specific affinity for the pulmonary vasculature and undergo fast inactivation and elimination from the blood. Lack of specificity for lung and short life-time in circulation limit the effectiveness of the conventionally administered therapy. Thus, results of worldwide clinical trials have documented several problems and limitations associated with fibrinolytic therapy using any of the known plasminogen activators, as well as their genetic variants and chemically modified forms (Prewitt, 1991; Verstraete and Lijnen, 1994; Lijnen and Collen, 1992; Fears and Poste, 1944).

Several approaches have been suggested to improve the therapeutic potential of plasminogen activators, including: 1) prolongation of the plasminogen activators life-time in the bloodstream (Kajihara *et al.*, 1994); 2) protection from inactivation by inhibitors (Runge *et al.*, 1991; Krishnamurti *et al.*, 1996); and 2) targeting to fibrin clots and thrombi. To achieve the last goal, plasminogen activators have been conjugated with mAb to fibrin (Lijnen and Collen, 1992) or with mAb recognizing epitopes presented on the surface of activated platelets (Runge *et al.*, 1991). Bi-specific antibodies possessing affinity for both the plasminogen activators and for fibrin have also been constructed with the goal of achieving selective accumulation of plasminogen activators in the fibrin clots (Lijnen and Collen, 1992). The therapeutic potential of these conjugates and mutant forms of plasminogen activators remains to be established. None of these approaches, however, provides accumulation of plasminogen activators in the pulmonary vasculature, the site where thrombi are likely to accumulate and cause morbidity. Local intrapulmonary delivery of fibrinolytics via catheter has been developed to attain high local concentration of plasmin in the pulmonary vasculature (Tapson *et al.*, 1994). However, plasminogen activators delivered by the catheter are rapidly removed from the pulmonary vasculature by the blood flow, thus limiting the period of time when high local concentration of plasminogen activator can be maintained after catheter removal. To

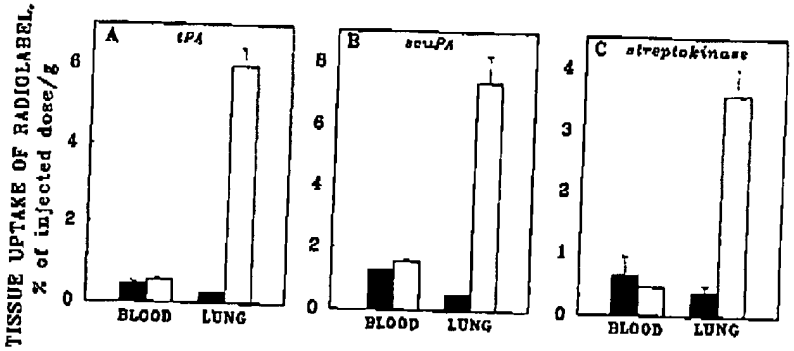

Fig. 7. Specific pulmonary targeting of plasminogen activators conjugated with monoclonal antibody to angiotensin-converting enzyme, anti-ACE mAb 9B9. Biotinylated radiolabeled tPA (A), scuPA (B) or streptokinase (C) were conjugated with anti-ACE mAb 9B9 (open bars) or with control mouse IgG (closed bars). Conjugates were injected i.v. in rats (1 μg/animal, three rats in each group). One hour after injection, radioactivity in blood and in lung tissue was determined by direct counting of blood or lung tissue in a gamma-counter. The data are presented as a percentage of injected dose per gram of tissue, mean ± S.D., $n = 3$.

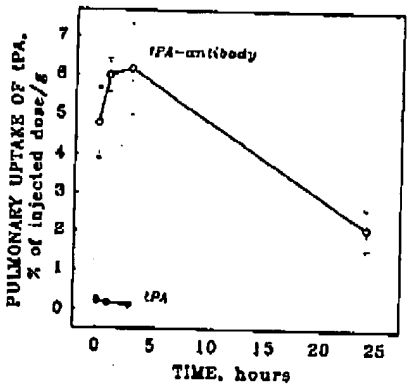

Fig. 8. Kinetics of the pulmonary uptake of tPA conjugated with anti-ACE mAb 9B9 after i.v. injection in rats. Radioactivity in the lungs was measured at indicated time after i.v. injection in rats of radiolabeled b-tPA conjugated with b-mAb 9B9 (open circles) or nonconjugated radiolabeled tPA (closed circles). The data are presented as a percentage of injected dose per gram of tissue (%ID/g), mean ± S.D., $n = 3$ rats in each group.

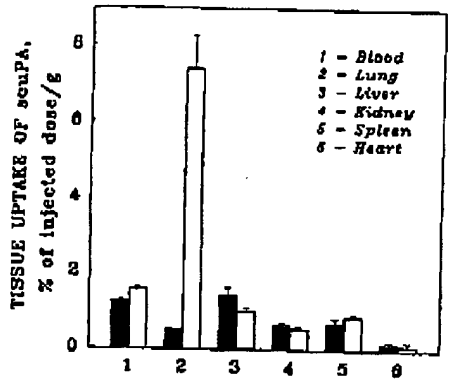

Fig. 9. Biodistribution of scuPA conjugated with anti-ACE mAb 9B9 after i.v. injection in rats. Radiolabeled biotinylated scuPA conjugated with anti-ACE mAb 9B9 (open bars) or with control IgG (closed bars) was injected in rats. One hour after injection, radioactivity in tissues was determined and expressed as a percentage of injected dose per gram of tissue (%ID/g). Mean ± S.D., $n = 3$ rats in each group.

overcome this obstacle, the plasminogen activator must have an affinity for the pulmonary vasculature. Therefore, conjugation of fibrinolytics with mAb recognizing the pulmonary endothelium represents a logical extension of previous studies in the field.

We have focused our efforts on conjugation of plasminogen activators with mAb against angiotensin-converting enzyme, anti-ACE mAb 9B9. During the previous decade we have explored this mAb and have documented that mAb 9B9, mouse IgG_1: 1) cross-reacts with human, monkey, rat, hamster and cat enzyme; 2) accumulates selectively in the lungs of these animal species after systemic administration and 3) does not fix complement, inhibit ACE enzyme activity, or induce toxic or pathological effects at a dose of 100 mg/kg (Danilov *et al.*, 1991, 1994; Muzykantov and Danilov, 1995). Specific pulmonary uptake of radiolabeled mAb 9B9 was characterized by gamma-scintigraphy in rats, monkeys and in humans (Muzykantov *et al.*, 1995). Coinjection of nonlabeled mAb 9B9 inhibits pulmonary uptake of radiolabeled mAb 9B9 in rats and hamsters, thus confirming specificity of targeting (Danilov *et al.*, 1991, 1994; Muzykantov and Danilov, 1995). Either intraarterial i.v. and i.p. injection in rats lead to pulmonary accumulation of radioactivity. Importantly, mAb 9B9 is retained in the lungs of animals for several days after i.v. injection (Danilov *et al.*, 1991, 1994; Muzykantov and Danilov, 1995). Glucose oxidase, catalase and superoxide dismutase conjugated with mAb 9B9 demonstrated selective pulmonary targeting after i.v. injection in rats (Muzykantov *et al.*, 1989, 1996a). Acute pulmonary injury in rats and pulmonary dissemination of tumor cells in hamsters led to detectable reduction of mAb 9B9 pulmonary uptake, but this reduction did not exceed 25 to 35% of the control level of mAb 9B9 pulmonary uptake and, thus did not compromise the targeting (Muzykantov and Danilov, 1995; Muzykantov *et al.*, 1991). Our preliminary clinical study shows that pulmonary uptake of ^{111}In-labeled mAb 9B9 is reduced, but still easily detectable in sarcoidosis patients (Muzykantov and Danilov, 1995). Therefore, mAb 9B9 accumulates in both normal and pathologically altered pulmonary vasculature and may be useful for selective pulmonary targeting of drugs and radiolabels in various animal species, including humans.

To develop a universal system for mAb 9B9-mediated pul-

monary targeting, we have explored streptavidin/biotin technology of protein conjugation. Streptavidin is a 60-kDa protein possessing four high affinity biotin-binding sites and the streptavidin/biotin pair is widely used in biomedicine as a cross-linking agent (Wilchek and Bayer, 1988). During the last decade, streptavidin-biotin technology has found *in vivo* applications for gamma-immunoscintigraphy (Khaw *et al.*, 1993) and for drug targeting (Muzykantov *et al.*, 1996a). Streptavidin is nontoxic and induces no harmful reactions in laboratory animals or in patients (Khaw *et al.*, 1993).

Results of *in vitro* studies shown in our paper demonstrate that: 1) biotinylation and subsequent interaction with streptavidin do not alter functional activity of plasminogen activators (fig. 3) and 2) targeting of biotinylated plasminogen activators provides effective local fibrinolysis despite steric limitations imposed by their immobilization on the target surface (Figs. 4 and 6). These results show that streptavidin/biotin cross-linker may be used as a general method for conjugation of plasminogen activators with a carrier antibody.

Results obtained *in vivo* in rats clearly demonstrate that mAb 9B9 may serve for targeting of plasminogen activators to the pulmonary vascular endothelium. All three plasminogen activators used in this study acquired an affinity for the pulmonary vasculature after conjugation with mAb 9B9. Systemic injection of mAb 9B9-conjugated plasminogen activators led to tissue-selective (lung/blood ratio 10 and higher), specific (no pulmonary uptake of IgG-conjugated plasminogen activators) and effective (up to 7% of injected dose per gram of the lung tissue) pulmonary targeting of plasminogen activators. Injection of nonmodified plasminogen activators or plasminogen activators conjugated with nonimmune IgG leads to the pulmonary uptake of 0.3 to 0.5% of injected dose. Therefore, pulmonary accumulation of mAb 9B9-conjugated plasminogen activators is 10 to 20 times higher than that of nonimmune counterparts 1 hr after systemic injection. Importantly, injection of mAb 9B9-conjugated plasminogen activator led to its prolonged retention in the lung tissue. Comparison of the surface areas under kinetic curves of the pulmonary uptake of mAb 9B9-conjugated tPA *vs.* nonconjugated tPA shows that conjugation with mAb 9B9 provides several orders of magnitude enhancement of the pulmonary delivery of plasminogen activator.

Therefore, presented data support our hypothesis that conjugation of plasminogen activators with anti-ACE mAb 9B9 provides an approach for the preferential pulmonary delivery and prolonged pulmonary retention of plasminogen activators. This provides a logical basis for the trial of fibrinolytic activity of mAb 9B9-conjugated plasminogen activators in animal models. In our study we injected in rats 1 μg of radiolabeled probes (plasminogen activators and antibody-conjugated plasminogen activators), to trace their biodistribution and pulmonary targeting. Our previous data show that injection of a saturating dose of mAb 9B9 (2–5 mg/rat) leads to accumulation of about 300 μg of antibody in the rat lung (Danilov *et al.*, 1991). Therefore, after injection of several milligrams of mAb 9B9-conjugated plasminogen activators we may expect accumulation of about 100 to 300 μg of plasminogen activator in the rat lung.

The fate of antibody-PA complex in the lung is important in terms of its therapeutic potential. Our recent results show that endothelium in cell culture internalize about 50% of cell-associated mAb 9B9 without marked degradation (Muzykantov *et al.*, 1996b). Therefore, a portion of the lung-targeted plasminogen activator may become inaccessible from the bloodstream. This would reduce its fibrinolytic potential. However, our results obtained in rats *in vivo* document that about 50% of the lung-accumulated radiolabeled mAb 9B9 remains associated with the lung plasma membrane fraction without marked degradation for at least several days after systemic injection (Muzykantov *et al.*, 1996b). Therefore, the fate of mAb 9B9 suggests that about half of mAb 9B9-conjugated plasminogen activators will be associated with endothelial plasma membrane in the lung tissue for a prolonged time after systemic injection.

This issue, as well as examination of the fibrinolytic potential of the lung-accumulated mAb 9B9-plasminogen activator complex, needs further experimental study. Our results document the targeting of the complex to the lung. Whether localization of functional plasminogen activator to the pulmonary endothelium will significantly enhance thrombolysis of pulmonary emboli remains to be determined.

Acknowledgments

The authors thank Drs. Douglas Cines and Harold Paleveky (University of Pennsylvania) for reading the manuscript and providing helpful discussion.

References

Barnathan, E., Kuo, A., van der Keyl, H., McCrae, K., Larsen, G. and Ciner, D.: Tissue-type plasminogen activator binding to human endothelial cells. Evidence for two distinct binding sites. J. Biol. Chem. **263**: 7792–7799, 1988.

Caldwell, P., Seegal, B., Hsu, K., Das, M. and Soffer, R.: Angiotensin-converting enzyme: vascular endothelial localization. Science **191**: 1050–1051, 1976.

Danilov, S., Muzykantov, V., Martynov, A., Atochina, E., Sakharov, I., Trakht, I. and Smirnov, V.: Lung is a target organ for monoclonal antibody to ACE. Lab. Invest. **64**: 118–124, 1991.

Danilov, S., Atochina, E., Hiemish, H., Churakova, T., Mildobayeva, A., Sakharov, I., Deichman, G., Ryan, U. and Muzykantov, V.: Interaction of monoclonal antibody to angiotensin-converting enzyme (ACE) with antigen *in vitro* and *in vivo*. Int. Immunol. **6**: 1131–1160, 1994.

Erdos, E.: Angiotensin-converting enzyme and changes of our concepts through the years. Hypertension **16**: 363–370, 1990.

Fears, R. and Poste, G.: Obstacles to the development of novel thrombolytic agents for acute myocardial infarction therapy. Fibrinolysis **8**: 203–213, 1944.

Higazi, A., Cohen, R., Henkin, J., Kniss, D., Schwartz, B. and Cines, D.: Enhancement of the enzymatic activity of single-chain urokinase plasminogen activator by soluble urokinase receptor. J. Biol. Chem. **270**: 17375–17380, 1995.

Kajihara, J., Shibata, K., Nakano, Y., Nishimuro, S. and Kato, K.: Physicochemical characterization of PEG-PPG conjugated human urokinase. Biochim. Biophys. Acta **1199**: 202–208, 1994.

Khaw, B., Strauss, H., Narula, J.: "Magic bullets": From muskets to smart bombs! J. Nuclear Med. **34**: 2264–2268, 1993.

Krishnamurti, C., Keyt, B., Maglasang, P. and Alving, B.: PAI-1-resistant tPA: Low doses prevent fibrin deposition in rabbits with increased PAI-1 activity. Blood **87**: 14–19, 1996.

Linnen, R. and Collen, D.: Remaining perspectives of mutant and chimeric plasminogen activators. Ann. N.Y. Acad. Sci. **667**: 357–364, 1992.

Muzykantov, V., Sakharov, D., Smirnov, M., Samokhin, G. and Smirnov, V.: Immunotargeting of erythrocyte-bound streptokinase provides local lysis of fibrin clot. Biochim. Biophys. Acta **884**: 355–363, 1986.

Muzykantov, V., Martynov, A., Puchinina, E. and Danilov, S.: In vivo administration of glucose oxidase conjugated with monoclonal antibody to human ACE. Am. Rev. Respir. Dis. **138**: 1464–1473, 1989.

Muzykantov, V., Puchinina, E., Atochina, E., Hiemish, H., Slinkin, M., Meertuk, F. and Danilov, S.: Endotoxin reduces specific pulmonary uptake of radiolabeled monoclonal antibody to ACE. J. Nuclear Med. **32**: 453–460, 1991.

Muzykantov, V., Atochina, E., Gavrilyuk, V., Danilov, S. and Fisher, A. B.: Immunotargeting of streptavidin to the pulmonary endothelium. J. Nuclear Med. **35**: 1358–1365, 1994.

MUZYKANTOV, V. AND DANILOV, S.: Targeting of radiolabeled monoclonal antibody against ACE to the pulmonary endothelium. *In* Targeted Delivery of Imaging Agents, ed. by V. Torchilin, pp. 465–485, Boca Raton, FL, CRC Press, 1995.

MUZYKANTOV, V., GAVRILUK, V., REINECKE, A., ATOCHINA, E., KUO, A., BARNATHAN, E. AND FISHER, A. B.: The functional effects of biotinylation of anti-ACE monoclonal antibody in terms of its targeting in vivo. Anal. Biochem. **226**: 279–287, 1995.

MUZYKANTOV, V., ATOCHINA, E., ISCHIROPOULOS, H., DANILOV, S. AND FISHER, A. B.: Immunotargeting of antioxidant enzymes to the pulmonary endothelium. Proc. Natl. Acad. Sci. U.S.A. **93**: 5213–5218, 1996.

MUZYKANTOV, V., ATOCHINA, E., KUO, A., BARNATHAN, E., NOTARFRANCESCO, K., SHUMAN, H., DODIA, C. AND FISHER, A. B.: Endothelial cells internalize monoclonal antibody to angiotensin-converting enzyme. Am. J. Physiol. **270**: L704–L713, 1996.

PLOW, E., HERREN, T., REDLITZ, A., MILES, L. AND HOOVER-PLOW, J.: The cell biology of plasminogen system. FASEB J. **9**: 939–945, 1995.

PREWITT, R.: Principles of thrombolysis in pulmonary embolism. Chest **99**: 157–164, 1991.

RUNGE, M., BODE, C., HABER, E. AND QUERTERMOUS, T.: Hybrid molecules: insights into plasminogen activator function. Mol. Biol. Med. **8**: 245–255, 1991.

SERRANO, R., RODRIGUEZ, P., PIZZO, S. AND GONZALEZ-GRONOW, M.: ATP-regulated activity of plasmin-streptokinase complex: a novel mechanism involving phosphorilation of streptokinase. Biochem. J. **318**: 171–177, 1996.

TAPSON, V., GURBEL, P., WITTY, L., PIEPER, K. AND STACK, R.: Pharmacomechanical thrombolysis of experimental pulmonary emboli. Chest **106**: 1558–1562, 1994.

VERSTRAETE, M. AND LIJNEN, H.: Novel thrombolytic agents. Cardiovasc. Drugs Therapy **8**: 801–811, 1994.

WILCHEK, M. AND BAYER, E.: The avidin-biotin complex in bioanalytical research. Anal. Biochem. **171**: 1–32, 1988.

Send reprint requests to: Dr. Vladimir R. Muzykantov, Institute for Environmental Medicine, University of Pennsylvania School of Medicine, One John Morgan Building, 36th Street and Hamilton Walk, Philadelphia, PA 19104-6068.

JPET PHARMACOLOGY AND EXPERIMENTAL THERAPEUTICS aspet